

People's Democratic Republic of Algeria
Ministry of Higher Education and Scientific Research
University of Kasdi Merbah, Ouargla

Faculty of New Technologies of Information and Communication

Department of Electronic and Telecommunications



Deep Neural Networks Improve Radiologists' Performance in Breast Cancer Screening

Thesis master degree in order to obtain a:

ACADEMIC MASTER

Domain: Science and technology

Field: Telecommunication

Specialty: Telecommunications systems

Presented by:

Anes medjouel & Bougueffa Eutamen hessen

Before the jury:

President	Khaled Bensid	MCB - Ouargla University
Examiner	Abdelhakim Chergui	MAB - Ouargla University
Examinatrice	Najla Betyab	MAB - Ouargla University
Supervisor	Azeddine BENLAMOUDI	MCA - Ouargla University

Academic Year: 2021 – 2022

Dedication Anes Medjouel

I dedicated this modest work to those who are dearest to me, I remember:

First all: my dears mother, No words can express their true value of gratitude and love who are the two dearest people in the world, may God protect and take care of them for me.

My father: my dears fathers, **Mouhammed Malek**. Who encouraged me in my academic path
"May God have mercy on him and make heaven his abode"

to My aunt: **Dalila Mahcen**.

To my brothers: **Bachir, Mostapha, and Mouhammed Tahar** .

To my sisters: **Oum Elhana, Sadjida, Aya and Alaa**

To my Colleague: Thank you for your patience and your love, I wish you a life full of success, happiness.

To my dear friends: **Billal Souigat, Bomedian Mefatih, Billal Cheriet, Achraf Ben dahou, Brahim Ghouar, Mohammed Larbi Snousi, Abe Moulode Mohammed** I can't find the sincere words to express my feelings and thoughts, you are my brothers.

To my teacher: **Hassani MOHAMED FOUAD**, thank you for help me during my studies at university.

My supervisor: **Dr Azeddine BENLAMOUDI**. May Allah grant your health and happiness and long life and make sure that I never fade away.

Dedication Bougueffa Eutamen Hessen

Praise to God who has enabled us for this which we would not have reached it if were not for the grace of God to us.

I dedicated this modest work to those who are dearest to me, I remember:

First of all: To my mother, no words can express their true value of gratitude and love for the two dearest people in the world. May God protect and take care of her for me.

To my Father: **Kamel**. Who encouraged me in my academic path

To my brothers: **Houssin, Abbas, Mouhammed**.

To my sisters: **Bensaadi Nourelhouda**

My colleague: thank you for your patience and your love, I wish you a life full of success, happiness.

To my dear friends: **Souici Akram, Geuchichi Hamza**, I can't find the sincere words to express my feelings and thoughts, you are my brothers.

My supervisor: **Dr Azeddine BENLAMOUDI**. May Allah grant your health and happiness and long life and make sure that I never fade away.

Acknowledgments

We owe a deep debt of gratitude to our Faculty of **Modern Information And Communication Technologies** and Department of **Electronic and Telecommunication** for allowing us to complete this work. We are grateful to some of the people who worked hard with us from the beginning to the completion of the current research. Our supervisor **Dr Azeddine BENLAMOUDI** was generous during all stages of the research. We would also like to thank the discussion committee headed by **Dr Khaled BENSID**, **Mr Abdelhakim CHERGUI**, and **Ms Najla BETYAB** Many thanks and appreciation to all of you. We would like to take this opportunity to express our sincere thanks to all our beloved friends and family, who have been so supportive all the way through doing our work. Finally, to everyone who contributed from near or far to completing this graduation project. First and foremost, we must acknowledge our infinite thanks to the Great God; Thankful for his help and blessings. We are sure that this work would not have been possible without his guidance.

Abstract

Machine learning has become a burgeoning field with a wide range of applications in both academia and industry. Breast cancer may be seen as a catalyst for incorporating the field of deep learning into the facilities of medical practitioners. Although it has not yet been widely adopted, it has sparked the curiosity of scientists. Because of this, it has brought attention to how these new technologies can be used in the medical field.

We show how advanced ways of analyzing medical images are changing, with a focus on global breast cancer updates. We also provide applications of deep learning in mammography. In addition, we discuss breast cancer and its effects on the world and how it motivates researchers to make innovations to fight this disease. Next, we put under scrutiny the proposed methods in the current literature that use deep learning in the field of diagnostics based on the *X-ray* medical imaging method.

In our experience, we used convolutional neural networks as one of the basic structures for deep learning, because they are the best in image analysis, we used BreakHis data containing 7909 breast cancer micro biopsy images, benign and malignant (5429 malignant, 2480 benign), in addition, we detail all the results of Our tests in this thesis.

Keywords

Computer Vision, Artificial Intelligence, Deep learning, Image processing, Mammography, Convolution Neural Network, Breast Cancer.

Résumé

L'apprentissage par machine est devenu un domaine en plein essor avec un large éventail d'applications à la fois dans le milieu universitaire et dans l'industrie. Le cancer du sein peut être considéré comme un catalyseur pour intégrer le domaine de l'apprentissage en profondeur dans les installations des médecins praticiens. Bien qu'elle ne soit pas encore largement adoptée, elle a suscité la curiosité des scientifiques. En conséquence, il a mis en évidence l'application de ces nouvelles technologies dans le domaine médical.

Nous donnons un aperçu de l'évolution des méthodes avancées d'analyse d'images médicales, avec un accent particulier sur les mises à jour mondiales sur le cancer du sein. Nous fournissons également des applications d'apprentissage en profondeur en mammographie. En outre, nous discutons du cancer du sein et de ses effets sur le monde, et de la manière dont il a motivé les chercheurs à innover pour lutter contre cette maladie. Ensuite, nous avons examiné les méthodes proposées dans la littérature actuelle qui utilisent l'apprentissage en profondeur dans le domaine du diagnostic basé sur la méthode d'imagerie médicale par rayons X.

Dans notre expérience, nous avons utilisé les réseaux de neurones convolutifs comme l'une des structures de base pour l'apprentissage en profondeur, car ils sont les meilleurs en analyse d'image, nous avons utilisé les données BreakHis contenant 7909 images de micro biopsie du cancer du sein, bénignes et malignes (5429 malignes, 2480 bénignes) , de plus, nous détaillons tous les résultats de Nos tests dans cette thèse.

Mote Clé

Vision par ordinateur, Intelligence Artificielle, Apprentissage en profondeur, Traitement d'images, Mammographie, Réseau de neurones à convolution, Cancer du sein.

المخلص:

أصبح التعلم الآلي مجالاً مزدهراً مع مجموعة واسعة من التطبيقات في كل من الأوساط الأكاديمية والصناعية. قد يُنظر إلى سرطان الثدي على أنه حافز لدمج مجال التعلم العميق في مرافق الممارسين الطبيين. على الرغم من أنه لم يتم اعتماده على نطاق واسع بعد ، فقد أثار فضول العلماء. ونتيجة لذلك ، فقد سلطت الضوء على تطبيق هذه التقنيات الجديدة في المجال الطبي.

نحن نقدم نظرة ثاقبة لتطوير الطرق المتقدمة لتحليل الصور الطبية ، مع التركيز بشكل خاص على تحديثات سرطان الثدي العالمية

كما نقدم تطبيقات التعلم العميق في التصوير الشعاعي للثدي. بالإضافة إلى ذلك ، نناقش سرطان الثدي وآثاره على العالم ، وكيف حفز الباحثين على ابتكار ابتكارات لمكلفة هذا المرض. بعد ذلك ، قمنا بفحص الأساليب المقترحة في الأدبيات الحالية التي تستخدم التعلم العميق في مجال التشخيص بناءً على طريقة التصوير الطبي بالأشعة السينية

في تجربتنا ، استخدمنا الشبكات العصبية التلافيفية كأحد الهياكل الأساسية للتعلم العميق ، لأنها الأفضل في تحليل الصور ، استخدمنا بيانات آبراك هيز التي تحتوي على ٧٩٠٩ صور خزعة صغيرة لسرطان الثدي ، حميدة وخبيثة (٥٤٢٩ خبيث ، ٢٤٨٠ حميدة) ، بالإضافة إلى ذلك ، نقوم بتفصيل جميع نتائج اختباراتنا في هذه الاطروحة.

الكلمات الدلالية:

الرؤية الحاسوبية ، الذكاء الاصطناعي ، التعلم العميق ، معالجة الصور ، تصوير الثدي بالأشعة ، الشبكة العصبية الالتفافية ، سرطان الثدي.

Contents

General introduction	1
1 Interpretation of mammography	2
1.1 Introduction	3
1.2 Structure of the breast	3
1.3 Breast cancer	4
1.4 Mammography	7
1.4.1 Impacts in mammography	12
1.5 Digital mammography	14
1.5.1 Image Acquisition	14
1.5.2 Image Storage	15
1.5.3 Image Display	16
1.6 Conclusion	17
2 Breast Cancer & CNN	18
2.1 Introduction	19
2.2 Breast cancer screening	19
2.3 Computer-Aided Detection/Diagnosis Computer-Aided Detection/Diagnosis (CAD) systems	19
2.3.1 Computer-aided detection	20
2.3.2 Computer-Aided Diagnosis	20
2.4 Diagnosis/detection support system for mammography	21
2.4.1 Mammography Preprocessing	22
2.4.2 Classification of breast tissue	22
2.4.3 Detection of an anomaly in Breast tissue	25
2.5 Convolution neural network	25
2.5.1 Input Layers	25
2.5.2 Convolutional Layers	26

2.5.3	Pooling Layers	27
2.5.4	Fully Connected Layers	28
2.6	Conclusion	29
3	Results and Discussion	30
3.1	Introduction	31
3.2	Proposed approach	31
3.2.1	Feature extraction	31
3.2.2	Classification	33
3.3	Database and protocol	34
3.4	Evaluation metrics	35
3.5	Results and Discussion	36
3.5.1	Effectiveness of number epochs	37
3.5.2	Effectiveness of Batch size and Learning rate	38
3.5.3	Effectiveness of optimizer	39
3.5.4	Compared with state of the art	40
3.6	Breast Cancer Detection Interface	42
3.7	Conclusion	44
	General conclusion	45

List of Figures

1.1	Illustration showing the breast anatomy	3
1.2	Latest stats	6
1.3	Age-standardized incidence (ASIR) and mortality (ASMR) rates per 100,000 population for female breast cancer in different countries in 2020.	8
1.4	Age-specific incidence rates of female breast cancer by different countries and HDI levels.	9
1.5	Age-specific mortality rates of female breast cancer by different countries and HDI levels.	10
1.6	An overview of mammography setup, where a women’s breast is placed on the breast support and a x-ray beam projection is generated in the x-ray tube (courtesy: Wikipedia).	11
1.7	A dedicated mammography system has many unique attributes, including K-edge filtration, collimation, and compression. Automatic Exposure Control (AEC) has an external or internal sensor for digital detectors and can be positioned by the user. Major components of a typical system, excluding the generator and user console, are shown.	12
1.8	Illustration showing the raw and processed mammogram in Full-Field Digital Mammography (FFDM).	13
1.9	Mammography projection views used in breast cancer screening studies: (a) shows the direction of two mostly used view points to produce mammograms, (b) CC view, and (c) MLO view	14
1.10	Schematic procedure of Digital Breast Tomosynthesis (DBT), showing the movement of the x-ray tube to acquire images at different angles. Note that the geometry differs between manufacturers	15
1.11	Sample DBT volume: Different slices of DBT volume traversing from left to right	16
2.1	The stages of the diagnostic/detection support system for mammography	22

2.2	A high-level overview of CNN Architecture	26
2.3	Input layer 3D volume	27
2.4	The convolution operation.	27
2.5	Max pooling on a single depth slice using a 2×2 filter with a stride of 2.	28
2.6	The output of the flattening operation is a vector.	28
3.1	The output of the flattening operation is a vector.	32
3.2	CNN Architecture.	33
3.3	Breast malignant tumor slides observed with different magnification ratio 40 X , 100 X , 200 X and 400 X.	34
3.4	Training accuracy and validation accuracy	37
3.5	Training loss and validation loss	37
3.6	Confusion matrix.	41
3.7	Graphical user interface	42
3.8	Sample Benign image for Testing	43
3.9	Sample Malignant image for Testing	43

List of Tables

1.1	The burden of breast cancer for different countries in 2020	5
2.1	Breast tissue density classification methods.	23
2.2	Breast tissue abnormality detection methods.	24
3.1	Parameters of the CNN architecture.	33
3.2	Details of fully connected network.	33
3.3	Distribution of images in dataset	35
3.4	Batch size	39
3.5	Learning Rate	39
3.6	Optimizers	40
3.7	Summary of result	40
3.8	Existing methods and respective Accuracy	41
3.9	Details of sample images from test set.	44
3.10	Prediction result	44

Acronyms

AEC	Automatic Exposure Control
AI	Artificial Intelligence
ANN	Artificial Neural Networks
CAD	Computer-Aided Detection/Diagnosis
CC	Craniocaudal View
CNN	Convolutional Neural Network
DBT	Digital Breast Tomosynthesis
DICOM	Digital Imaging and Communications in Medicine
FDA	Food and Drug Administration
FFDM	Full-Field Digital Mammography
FN	Flase Negative
FP	False Positive
HDI	Human Development Index
HS	Harmony Search
IARC	International Agency for Research on Cancer
KNN	K-nearest Neighbor Classifiers
MLO	Mediolateral Oblique
PACS	Picture Archiving and Communication System
RGB	Red Green Blue
RLE	Run-length Encoding
RNN	Recurrent Neural Networks
ReLU	Rectified Linear Unit

SFM	Screen-Film Mammography
SVM	Support Vector Machine
TN	True Negative
TP	True positive

General Introduction

Due to scientific breakthroughs and constantly developing infrastructure, machine learning has seen huge success in a variety of industries over the past decade. Models such as artificial neural networks require huge amounts of computing, which can now be addressed by models such as machine learning. Recent attempts have shown promise in improving detection in a range of medical fields, including diagnosis and prognosis.

The terrible severity and prevalence of breast cancer can be considered to bring deep learning into the clinics of medical practitioners. Even if it is not yet widely applied, it has become of interest to researchers all over the world. Commercial applications have seized the opportunity to promote their solutions, and artificial intelligence technology has become a catalyst for any future diseases or epidemics. At the radiographic level, it is time to put current structures and potential future innovations to use in the service of human well-being.

In this work, we provide a reflection on the latest emerging technologies in the field of medical image analysis, with a main focus on the updates brought by breast cancer. This thesis is organized into three chapters: In the first chapter 1, we present the statistical and medical risk of breast cancer and also the interpretation of mammography. In the second chapter 2, we delve into the world of deep learning and review its application in mammography. The last chapter 3 covers the analysis and comparison of the proposed methods in the recent literature that apply deep learning in the field and presents the results obtained. Finally, we will draw conclusions from our findings and discuss how we can improve them in the future.

1

Interpretation of mammography

1.1 Introduction

Mammograms are X-ray images of the breasts designed to detect cancer cells and other changes in breast tissue, there two types of mammograms that we perform one is in the screening setting and the others in the diagnostic centre in general screening mammograms are performed in all women every one to two years after the age of 40. In this chapter, we will review what breast cancer is, in addition to highlighting the mammogram and its effects.

1.2 Structure of the breast

The breast is a complicated structure that is made up of 15 to 20 lobes. Each lobe is made up of lobules, which are tiny structures. The lobules are grouped in clusters, with small "bulbs" that generate milk at the end of each lobule. The lobes, lobules, and bulbs are joined by ducts, which are tiny tubes [1].

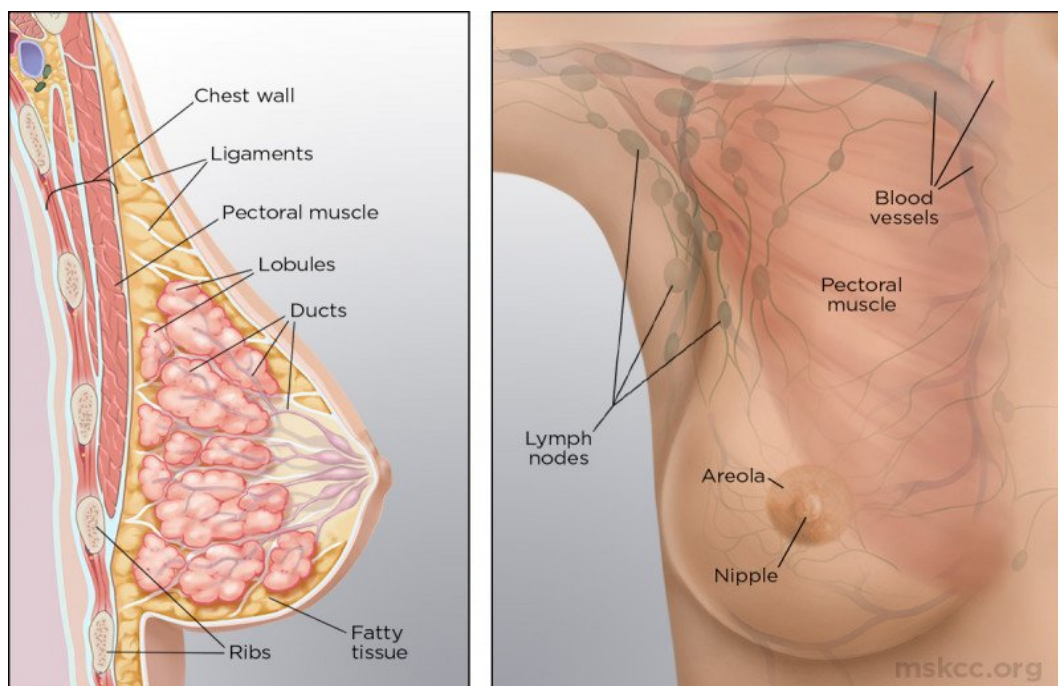


Figure 1.1: Illustration showing the breast anatomy

[2]

Milk is carried to the nipples, which are positioned in the center of the areola, through

the ducts (the darker area surrounding the nipple). Fats fill the gaps between the lobes and the ducts. The breast anatomy is depicted in fig 1.1, which shows the internal structure of the breast. Different forms of fatty, fibrous, and glandular tissue can be found in the female breasts:

- The breast lobes and breast ducts are glandular tissue.
- Ligaments, supporting tissues (dense breast tissue), and scar tissues all fall under the category of fibrous tissues.
- Breast size is mostly determined by fatty tissue (non-dense breast tissue), which fills in the crevices between glandular and fibrous tissue.

All non-fatty tissue is referred to as fibroglandular tissue. In addition, ligaments are supporting, flexible connective tissue bands that reach from the skin to the chest wall to keep the breast tissue in place. The pectoral muscle supports both breasts by lying against the chest wall below them. Furthermore, because each woman's breast has a unique blend of fatty and dense tissue, no two women's breasts are same. Some women's breasts are nearly entirely made up of fatty tissue, while others have a mixture of fatty and fibroglandular tissue. The amount of fatty tissue in women's breasts grows with age, such that by the age of 70, roughly 80 of all women's breasts are made up largely of fatty tissues. Breast cancer may develop in any area of the breast, thus women need to be screened with the right imaging tools [1].

1.3 Breast cancer

In the female population, breast cancer is the most frequent type of cancer. Approximately 12% of women in the United States will be diagnosed with breast cancer at some point throughout their lives. Breast cancer will affect 2.3 million women globally in 2020, with 685,000 fatalities. Breast cancer has been diagnosed in 7.8 million women According to the latest statistics (See Fig. 1.2), making it the most common disease in the world. Breast cancer causes more disability adjusted life years (DALYs) in women throughout the world than any other kind of cancer. Breast cancer strikes women at any age after puberty in every nation on the planet, with rates rising as they become older. The International Agency for Research on Cancer (IARC)

Country/ Region		Incidence					Mortality		
		Propotion					Propotion	Crude	
		Cases	(%)	Crude Rate	ASIR	Deaths	(%)	Rate	ASMR
World		2,261,419	100.0	58.5	47.8	684,996	100.0	17.7	13.6
Human Development Index (HDI)									
HDI	Very high HDI	1,017,459	45.0	128.7	75.6	231,093	33.8	29.2	13.4
	High HDI	825,438	36.5	57.2	42.7	247,486	36.2	17.2	12.1
	Medium HDI	307,658	13.6	27.1	27.8	147,427	21.5	13.0	13.6
	Low HDI	109,572	4.8	22.2	36.1	58,586	8.6	11.8	20.1
Asia		1,026,171	45.4	45.3	36.8	346,009	50.5	15.3	11.9
Asia	China	416,371	18.4	59.0	39.1	117,174	17.1	16.6	9.5
	Japan	92,024	4.1	76.3	76.3	17,081	2.5	26.4	9.9
	South Korea	25,814	1.1	100.8	64.2	3,009	0.4	11.8	6.4
	Iran	16,967	0.8	40.8	35.8	4,81	0.7	11.6	10.8
	Zionist occupation	4,348	0.2	100.0	78.3	1,194	0.2	27.5	16.7
	Singapore	3,662	0.2	131.3	77.9	921	0.1	33.0	17.8
Europe		531,086	23.5	137.2	74.3	141,765	20.7	36.6	14.8
Europe	United Kingdom	53,889	2.4	156.9	87.7	11,839	1.7	34.5	14.0
	Denmark	5,083	0.2	174.5	98.4	1,121	0.2	38.5	14.9
	Italy	55,133	2.4	177.7	87.0	12,633	1.8	40.7	13.4
	Belgium	11,734	0.5	200.7	113.2	2,362	0.3	40.4	15.1
	Hungary	7,565	0.3	149.4	77.3	2,195	0.3	43.4	17.3
	Africa	186,598	8.3	27.8	40.7	85,787	12.5	12.8	19.4
	South Africa	15,491	0.7	51.5	52.6	4,664	0.7	15.5	16.0
	Morocco	11,747	0.5	63.2	56.4	3,695	0.5	19.9	17.5
	Cameroon	4,17	0.2	31.4	43.6	2,108	0.3	15.9	22.8
	Nigeria	28,38	1.3	27.9	49.0	14,274	2.1	14.0	25.5
	Mauritius	648	0.0	100.6	66.2	207	0.0	32.1	20.0
Oceania		25,873	1.1	121.4	87.8	5,044	0.7	23.7	14.7
Oceania	Australia	19,617	0.9	153.2	96.0	3,132	0.5	24.5	11.7
	Fiji	302	0.0	68.3	65.1	184	0.0	41.6	41.0
	Samoa	66	0.0	69.0	81.4	21	0.0	21.9	25.6
America		491,691	21.7	94.8	68.0	106,391	15.5	20.5	13.2
	USA	253,465	11.2	151.6	90.3	42,617	6.2	25.5	12.4
	Mexico	29,929	1.3	45.4	40.5	7,931	1.2	12.0	10.6
	Argentina	22,024	1.0	95.1	73.1	6,821	1.0	29.5	18.9
	Costa Rica	1,624	0.1	63.7	47.5	433	0.1	17.0	11.5
	Jamaica	1,208	0.1	81.0	66.9	637	0.1	42.7	34.1

Table 1.1: The burden of breast cancer for different countries in 2020
[3]

estimates that globally, 1 in 5 people develop cancer during their lifetime, and 1 in 8 men and 1 in 11 women die from the disease. These new estimates suggest that more than 50 million people are living within five years of a past cancer diagnosis. Aging populations globally and socio-economic risk factors remain among the primary factors driving this increase.

Breast cancer represents 1 in 4 cancers diagnosed among women globally. Colorectal, lung, cervical, and thyroid cancers are also common among women [1].

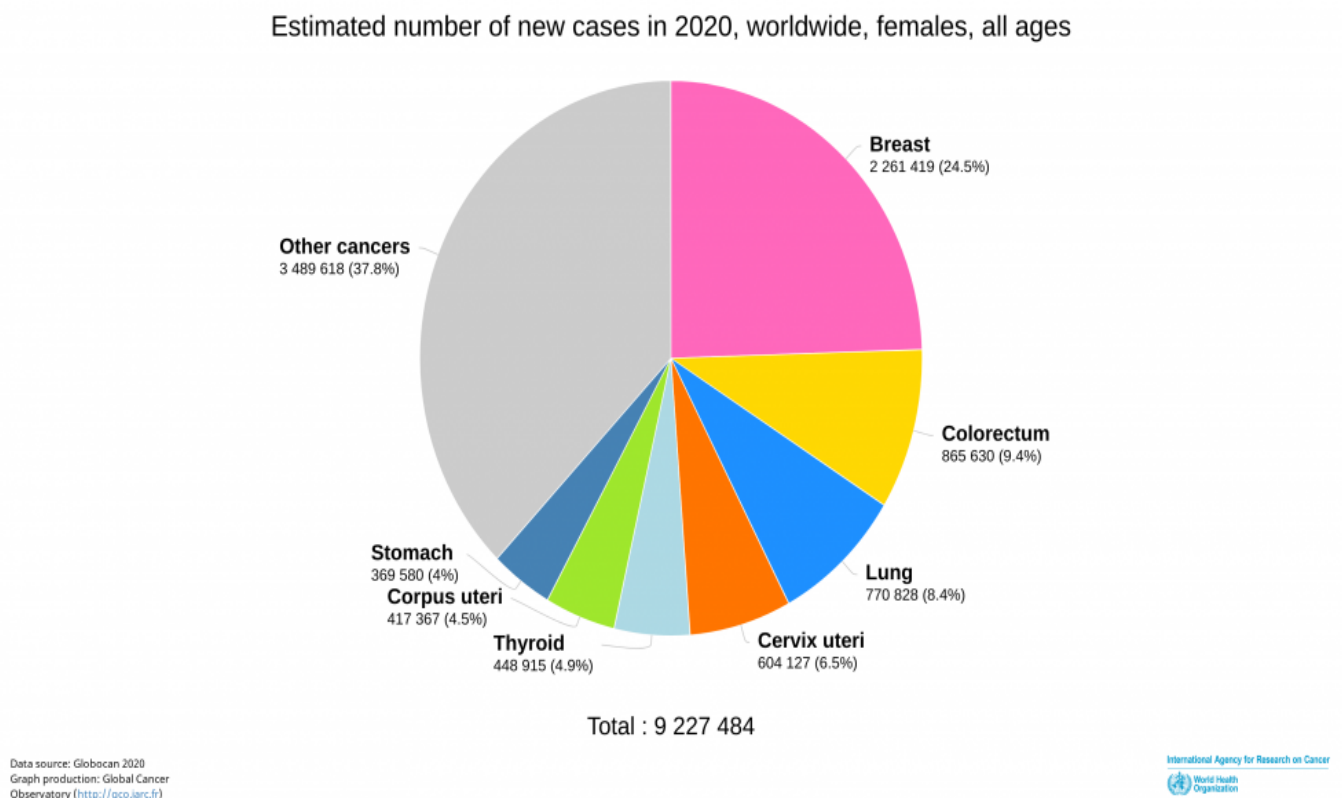


Figure 1.2: Latest stats

Breast cancer incidence rates were 58.5 and 47.8 per 100,000 people, respectively, when age was taken into account (See Table 1.1, Figure 1.3). China had the highest number of breast cancer cases, accounting for around 18.4% of worldwide breast cancer cases, followed by the United States, which had 11.8% of global breast cancer cases (See Table 1.1). The age-standardized incidence rates differed by more than thrice, ranging from 113.2 per 100,000 people in Belgium to 35.8 per 100,000 in Iran (See Table 1.1, Figure 1.3). Highly developed countries (Belgium, Denmark, Australia, the United States, the United Kingdom, and Italy)

had much higher incidence rates (47.8 per 100,000 population) than developing countries (Iran, China, Mexico, Cameroon, and Costa Rica), while developing countries (Iran, China, Mexico, Cameroon, and Costa Rica) had much lower incidence rates (See Table 1.1, Figure 1.3). In all nations studied, the age-specific incidence rates of breast cancer were relatively low for females under 25 years old, but increased rapidly after this age (See Figure 1.4). Surprisingly, the peak age of breast cancer was different in different parts of the world. The youngest onset peak age was 40 years old in South Korea and Cameroon (See Figure 1.4). Females aged 55-60 years old were most interested in China, Japan, Iran, Fiji, and Morocco. The peak beginning age of breast cancer in the United States, Belgium, Australia, and the United Kingdom was 70 years old (See Figure 1.4) [3].

Breast cancer claimed the lives of around 685,000 women in 2020, accounting for roughly 15.5 percent of all cancer fatalities worldwide. Breast cancer had crude and age-standardized death rates of 17.7 and 13.6 per 100,000 people worldwide, respectively (See Table 1.1, figure 1.3). Similar to the high number of breast cancer cases, China had the highest number of breast cancer fatalities, accounting for 17.1% of all cancer deaths worldwide, followed by the United States, which accounted for 6.2 percent of all breast cancer deaths worldwide (See Table 1.1). The age-standardized death rates differed dramatically (almost seven-fold) between nations, ranging from 41.0 per 100,000 in Fiji to 6.4 per 100,000 in South Korea. In contrast to the incidence rates, most poor or developing nations (such as Fiji, Jamaica, Samoa, Nigeria, and Cameroon) had high death rates, whereas high-income countries (such as South Korea, Japan, and the United States) had lower mortality rates (See Table 1.1, Figure 1.3). Breast cancer death rates increased with age in most of the nations studied, peaking around 70 years old (See Figure 1.5) [3].

1.4 Mammography

Mammography is a technique for early detection of breast cancer that uses a low-dose x-ray to project the breast's interior tissues. Signs will be more visible in this manner. The presence of malignancy (masses, microcalcifications, asymmetries, and deformities) might be a sign of

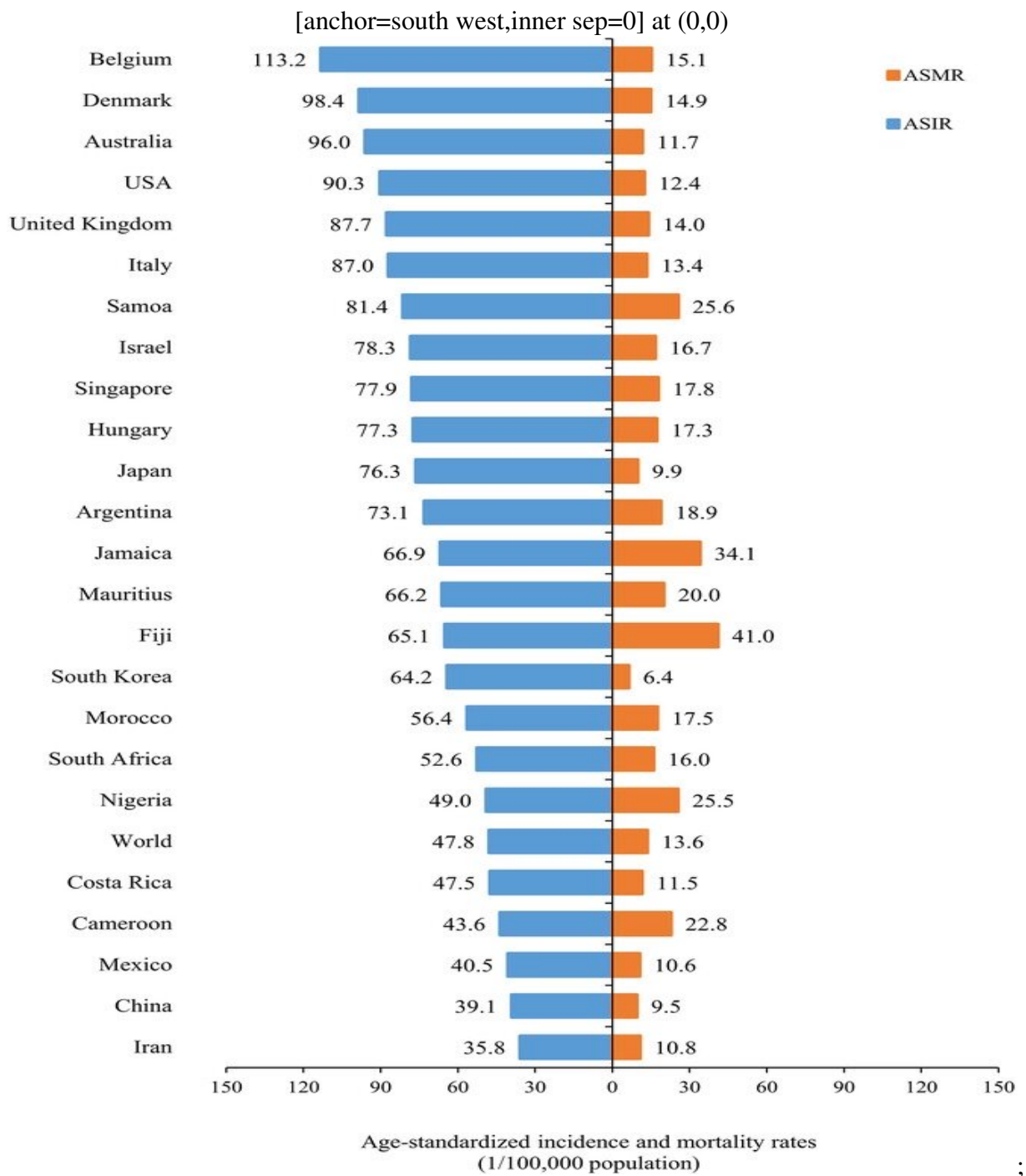


Figure 1.3: Age-standardized incidence (ASIR) and mortality (ASMR) rates per 100,000 population for female breast cancer in different countries in 2020.

[3]

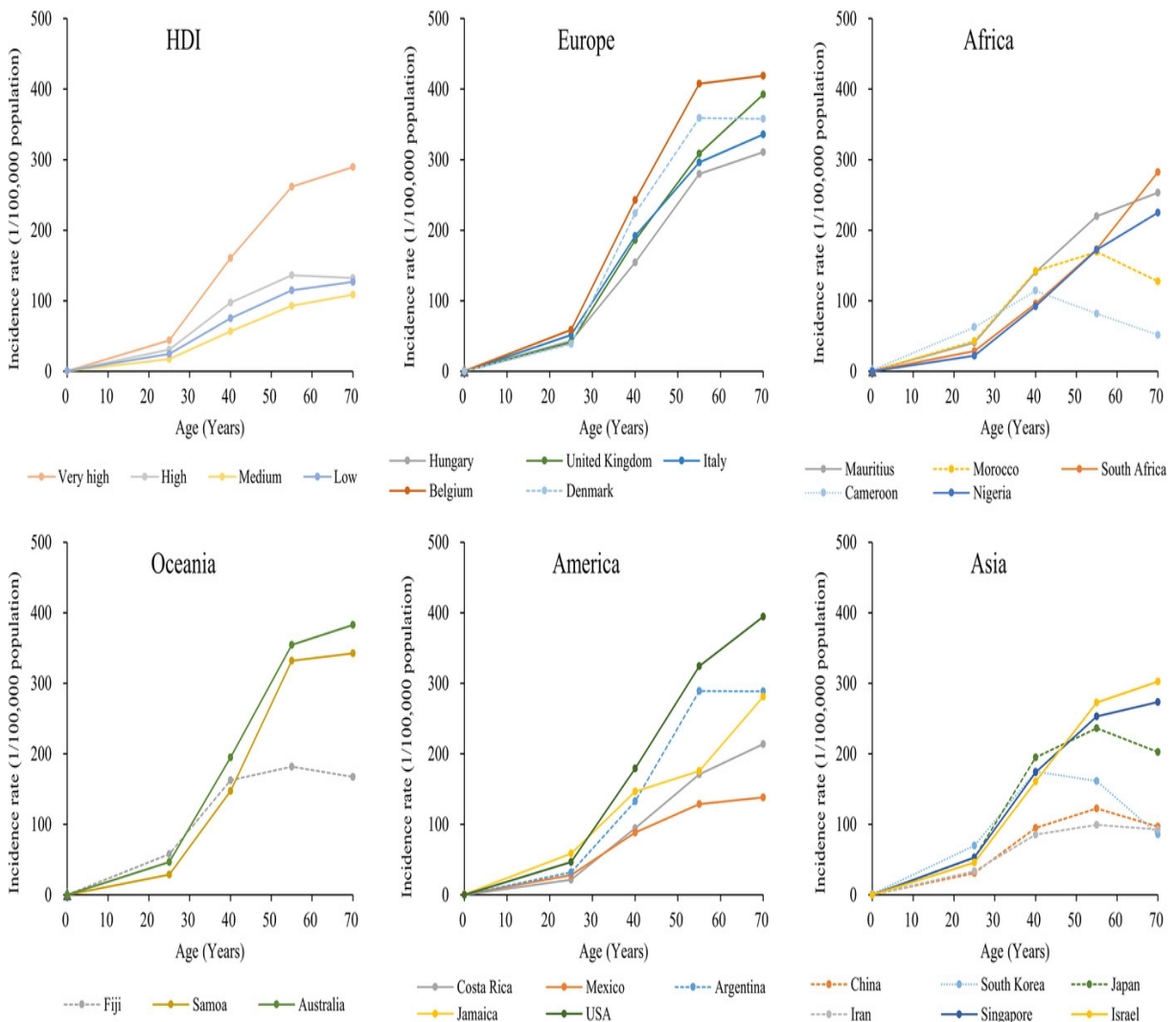


Figure 1.4: Age-specific incidence rates of female breast cancer by different countries and HDI levels. [3]

malignancy visualised. Figures 1.6 and 1.7 depicts an example of a mammography system. The breast is sandwiched between the compression plate and the breast support, and then, from the top, they were subjected to low-intensity x-ray beams (x-ray tube). The x-ray photons generated in the tube are captured by an image receptor placed beneath the breast support. In addition, an anti-scatter grid is usually placed between the breast support and the detector to decrease scattered radiation signal, which lowers picture contrast. The scanners produce raw and processed mammograms as shown in Figure 1.8 [1].

The most generally used procedure for breast cancer screening is mammography, which is

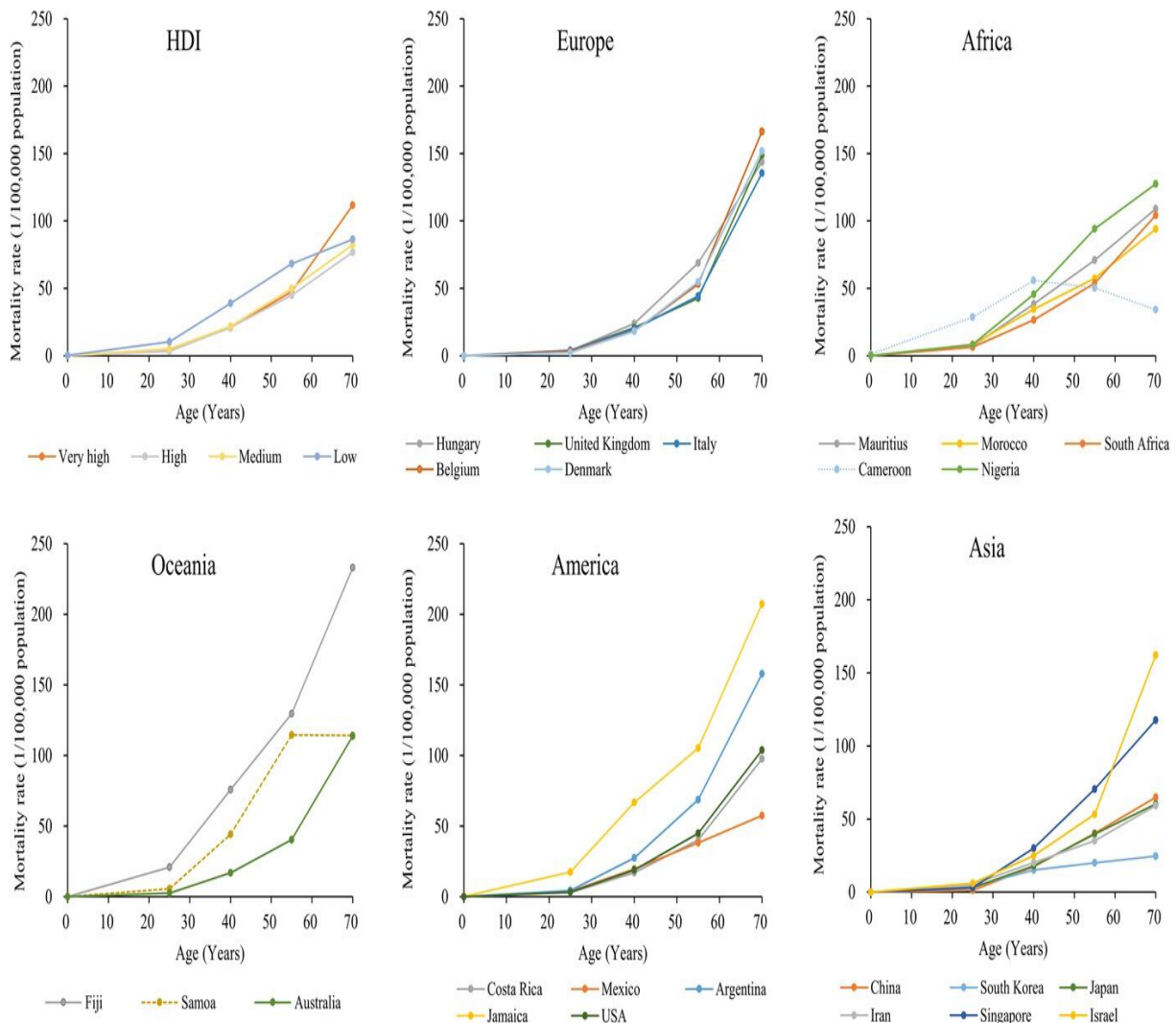


Figure 1.5: Age-specific mortality rates of female breast cancer by different countries and HDI levels. [3]

quick, inexpensive, and does not require a highly competent operator. However, there are a number of drawbacks to using this method. It has a high risk of False Negatives (FN: detection shows that there is no cancer but there is a cancer) and False Positives (FP: detection reveals certain cancer signs (tumour or micro-calcifications) although there is no cancer) in particular female demographic groups (with thick breasts). A woman with no disease is biopsied in the latter, but a woman with disease is left untreated and can result in a fatality in the former [1].

Each breast is obtained utilizing two separate view points (Craniocaudal View (CC) and Mediolateral Oblique (MLO)) in mammography-based screening programs, as shown in Fig.

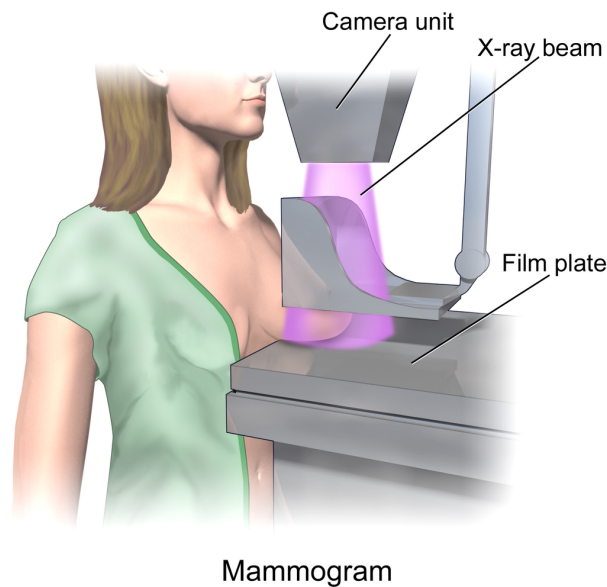


Figure 1.6: An overview of mammography setup, where a women's breast is placed on the breast support and a x-ray beam projection is generated in the x-ray tube (courtesy: Wikipedia).

1.9 a. Sample mammograms from these two view positions are displayed in Figures 1.9 b and 1.9 c. If the radiologist notices questionable areas, further image projections (e.g. enlarged views, medio-lateral views) might be done. Screen-Film Mammography (SFM) employed photographic films to capture the breast scan in the past. With advances in imaging technology, high-quality FFDM are now employed, which may be viewed immediately on computers. To address the issues with standard 2D mammography, pseudo-3D DBT has exploded in popularity in recent years as a novel imaging method for reducing the masking impact of overlapping fibro-glandular tissue and thereby enhancing breast cancer detection. The x-ray tube passes through a narrow arc above the breast (See Fig. 1.10) and several low-dose x-rays are taken [1].

Exposures are taken, which are subsequently post-processed to produce pseudo-3D breast volumes. Each slice of this pseudo-3D volume represents a breast depth. Slices are usually spaced by 1 mm, allowing for improved visualization of the interior breast tissue and reducing the overlapping effects seen in mammography. Varying DBT geometries and acquisition settings (e.g., narrow vs. broad angle) are available, with different detection performance in masses and microcalcifications. Figure 1.11 displays different slices of breast DBT volume as an example. Despite the growing use of DBT, x-ray mammography remains the gold standard

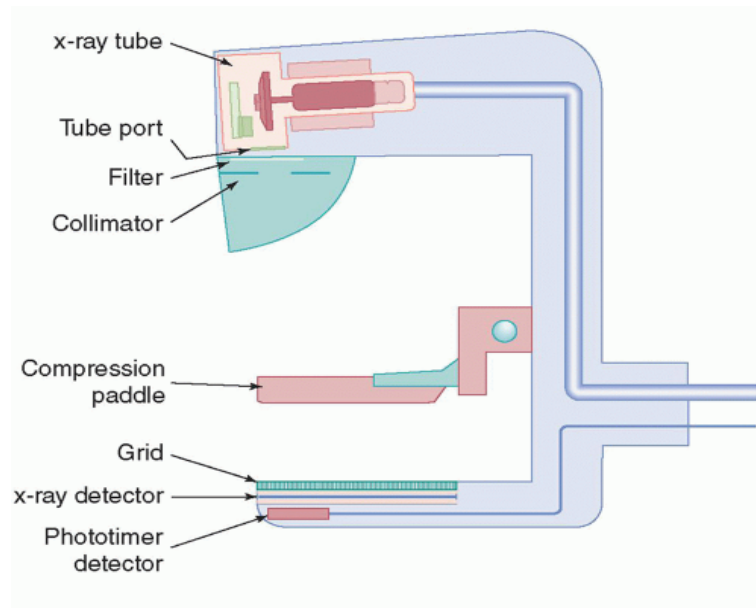


Figure 1.7: A dedicated mammography system has many unique attributes, including K-edge filtration, collimation, and compression. AEC has an external or internal sensor for digital detectors and can be positioned by the user. Major components of a typical system, excluding the generator and user console, are shown.

[4]

imaging modality for breast cancer screening due to its speed and cost effectiveness. Furthermore, DBT is a relatively new treatment option, with limited access in hospitals. As a result, it is not yet regarded as a standard approach for breast cancer detection [1].

1.4.1 Impacts in mammography

- exposure to radiation, Exposure to small amounts of radiation however, for many women, the benefits of a regular mammogram far outweigh the risks associated with the amount of radiation they receive.
- Not always accurate, the accuracy of the procedure depends in part on the technique used and the experience and skills of the radiologist.
- Other factors (such as age and breast density) can cause a "fake" mammogram, Negative or Positive
- Difficult to use for young people, the breasts of younger women contain more glands

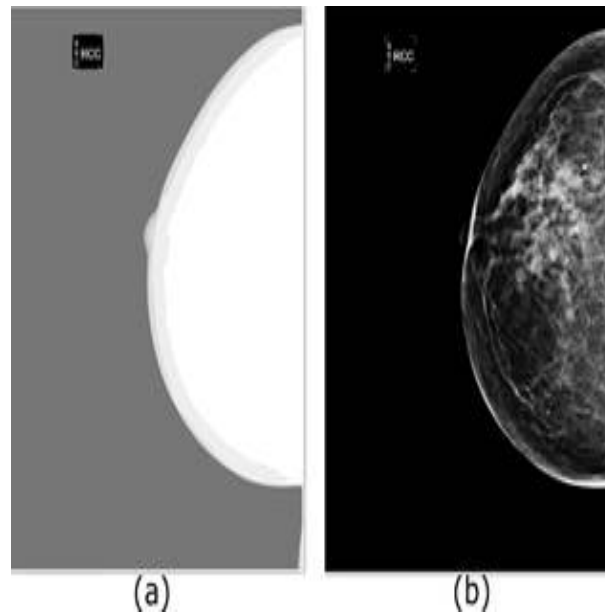


Figure 1.8: Illustration showing the raw and processed mammogram in FFDM.

and ligaments than the breasts of older people, therefore, dense breast tissue can mask the signs of cancer, but as you get older, there will be more fat in the breast tissue and the glands will become less, therefore, it becomes easier to detect breast changes with a mammogram.

- The need for more tests, among women of all ages who undergo mammograms, about 10% of women require additional tests, such as ultrasound and biopsy, A sample of breast tissue is collected in a laboratory examination, most abnormal findings are not cancerous.
- If there is an abnormality on the mammogram, the radiologist needs to compare it with the previous mammogram.
- It cannot detect all cancers, some cancers found through a physical exam don't show up on a mammogram, the cancer may be small or located in areas that are difficult to show on a mammogram, like armpits.
- Not all cancers detected through it can be cured, some types of cancer are dangerous because they grow quickly and spread to other parts of the body early.
- Damage to the fetus, these rays may harm the fetus, which requires telling the doctor if

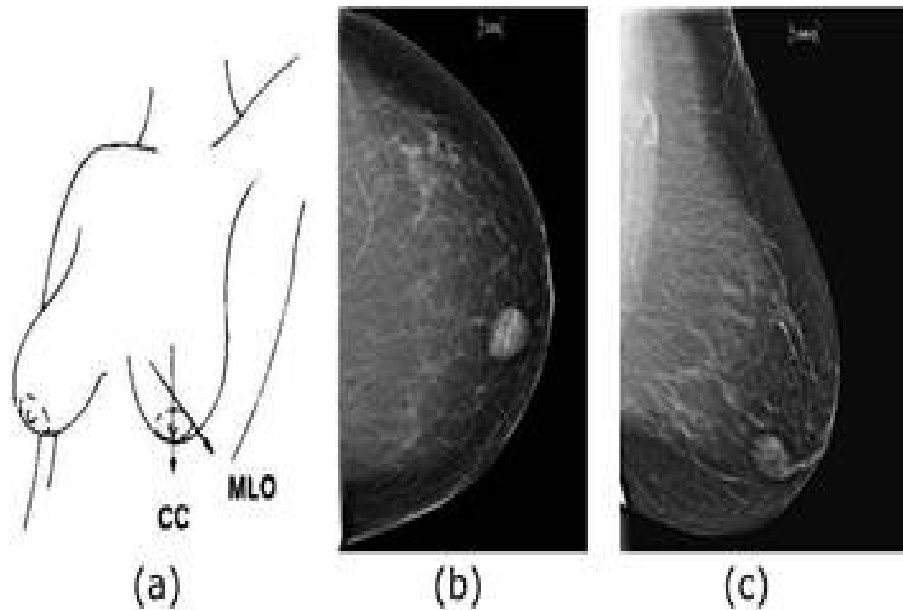


Figure 1.9: Mammography projection views used in breast cancer screening studies: (a) shows the direction of two mostly used view points to produce mammograms, (b) CC view, and (c) MLO view

the woman is pregnant [5].

1.5 Digital mammography

As a result of the digital revolution, conventional film-based hospitals are switching to digital hospitals, where clinicians may access patient medical data, chart information, and test results electronically from anywhere in the hospital. In this regard, full-digital mammography is gaining traction in comparison to the still-popular film-screen mammography, because digital acquisition, storage, and display procedures may all be separated and optimized separately. Let us go through these processes in further detail [6].

1.5.1 Image Acquisition

Traditional screen-film receptors have lower quantum efficiency and resolution than digital detectors. These will result in lower doses and better picture quality in mammography. According to how the X-ray is collected, digital detectors for mammography can be classified as

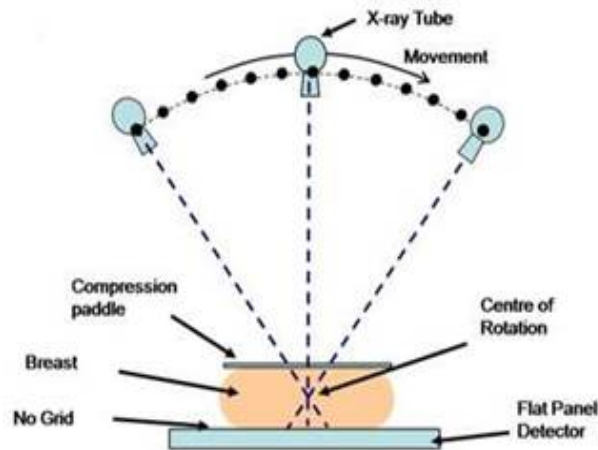


Figure 1.10: Schematic procedure of DBT, showing the movement of the x-ray tube to acquire images at different angles. Note that the geometry differs between manufacturers

indirect or direct conversion detectors. The energy of the X-rays is caught by a scintillator, which transforms it to light in indirect conversion methods (the first ones). Following that, an array of thin film diodes captures the light and converts it to an electrical signal, which is then caught by thin-film transistors. The fundamental issue with these systems is that the scintillator's generated light scatters, causing the same X-ray to be collected by many transistors. In direct conversion devices, on the other hand, the same photo-conductor that captures the X-ray can also create an electrical signal. As a result, dispersion in these systems is less severe. Berns *et al.* [7] compared the acquisition times of digital mammography with screen-film mammography. While the former took an average of 21.6 minutes, the latter took just 14.1 minutes, a remarkable 35 percent less time. The specialists took an average of 1.4 minutes to analyze the pictures for screen-film mammography and 2.3 minutes for digital mammography, a significant 57 percent greater interpretation time [6].

1.5.2 Image Storage

After the image has been captured, it must be saved. The Digital Imaging and Communications in Medicine (DICOM) standard to do this. This standard covers not only the storing of information in medical imaging, but also the printing and transfer of it. The DICOM format varies from the others in that it combines information on the patient and the image source (in

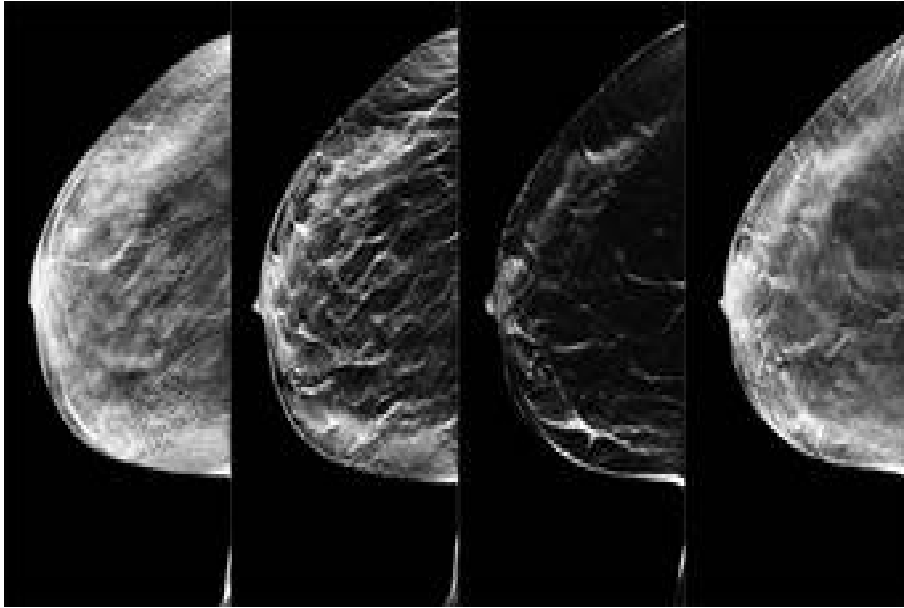


Figure 1.11: Sample DBT volume: Different slices of DBT volume traversing from left to right

our example, a mammogram), as well as the entire picture or images. As a result, photographs from a single research are never incorrectly separated from their associated data. JPEG, JPEG Lossless, JPEG 2000, and Run-length encoding are some of the standards that may be used to compress picture data Run-length Encoding (RLE). The paper by Avrin *et al.* [8] includes a discussion of its utility. They believe that the benefits of adopting compression techniques over expanding existing and future technology's storing capacity are not as evident. Furthermore, the DICOM standard controls the communication protocol, allowing the hospital's many imaging instruments to be integrated. As a result, monitors, scanners, servers, workstations, printers, and network gear may all be linked into a completely digital system known as the Picture Archiving and Communication System (PACS). A PACS network is typically made up of a central server that stores the DICOM database and a series of clients that give or consume the pictures [6].

1.5.3 Image Display

The picture from the digital mammogram can be forwarded to the screening workstation, where one or more professionals would generally examine and diagnose the case once it has been received and saved by the PACS database. In contrast to a traditional movie screen, the

experts will have to see the image on an electronic display (also called soft-copy display). Soft-copy reading, as opposed to (static) film reading, provides more options. Experiments have demonstrated that presenting current and previous mammograms on the same screen allows for a better assessment of temporal changes than displaying pictures adjacent to each other, especially if the images are appropriately registered in the spatial and gray-scale domains. The biggest disadvantage is that a malfunctioning, under-calibrated, or incorrectly set-up display can degrade the overall quality of a diagnostic operation. Clinical trials suggest that radiologists can interpret digital screening mammography as well as conventional films using soft-copy reading, with no significant variations in sensitivity or specificity. Furthermore, both investigations reveal that the speed of interpretation did not change much (in contrast to the already cited work of Berns *et al.* [6]).

1.6 Conclusion

Due to the complexities of breast structure and the difficulty of mammography in detecting cancer, this has led to its widespread, which prompted scientists and researchers to research and devise a method of mammography to aid in early detection, which led to these efforts to reach mammography. Regular mammograms are the best tests doctors have to find breast cancer early, sometimes up to three years before it can be felt, We also learned about the risks of mammography and its impact on women.

2

Breast Cancer & CNN

2.1 Introduction

Breast cancer is the second most frequent cancer in women and the primary cause of mortality from cancer. It has evolved into a severe worldwide health concern during the last 50 years, with its prevalence growing in recent years. If breast cancer is detected early, it can be diagnosed and treated more successfully. Using deep learning, CAD devices can aid in the early diagnosis of breast cancer and minimize mortality among breast cancer patients.

The synergistic neural network was chosen because it has shown good performance in a variety of computer vision and machine learning challenges. Thanks to the ways in which the synaptic neural network works, many powerful research papers have been published on this issue, which greatly help reduce the time it takes radiologists to diagnose a patient's condition (healthy or ill)

2.2 Breast cancer screening

Breast cancer screening is examining a woman's breast before she develops signs of the disease. Screening can take several forms; a mammogram is an X-ray scan of the breast. This picture is examined by a radiologist for abnormal findings. A clinical breast exam is a physical examination of the breasts performed by a doctor or nurse who uses their hands to feel for lumps or other changes. Women can also do a breast self-exam, which involves inspecting their own breasts for lumps or changes in the breasts or underarm. Breast cancer is best detected early, before symptoms occur, with mammograms. Breast cancer can be treated more easily if it is detected early. Digital mammography is becoming the most often used technology. The breast X-ray pictures can be taken on film or saved immediately to a computer. There are no changes in how a mammography and a digital mammogram are interpreted [9].

2.3 Computer-Aided Detection/Diagnosis CAD systems

A CAD system analyzes medical pictures and assists the detection specialist. It is frequently used as a detector and a classifier (K-nearest Neighbor Classifiers (KNN), decision trees, etc.).

The earliest studies on automatic mammography processing systems attempted to provide radiologists with a second interpretation to aid them in early detection and diagnosis. The use of CAD technologies might increase radiologists' performance in breast cancer screening [10].

2.3.1 Computer-aided detection

On traditional mammography, the rate of false negative interpretations is quite high (between 10% and 30%). As a result, computer-assisted detection is becoming more widely employed in mammography screening, as it enhances mammogram sensitivity. A scanner converts the film mammography picture into a digital image. A computer analyzes the digital image and displays it on the screen. Software is used to scan the image and offer messages in computer-aided detection. Using information derived from mammography, the detector detects anomalies. The role of the classifier is to sort.

CAD (Computer-aided Detection) is a helpful addition to the radiologist's toolkit. Expert radiologists must choose a CAD with the most efficient algorithms, especially when it comes to mass detection. Given the potential benefits of these technologies, the Food and Drug Administration (FDA) has approved four computer-aided detection systems in the United States since 1998. The R2 Image Checker is the first system created. In January 2002, two were approved: the CADx Second Look and the CAD MammoReader. These two companies ended up merging and they kept the name of Second Look. Then the "Kodak DirectView CR" Mammography Feature system was released [10].

2.3.2 Computer-Aided Diagnosis

The diagnosis comes from the Greek "diagnosis": knowledge. Originally used in the medical field, this term means the identification of a disease by its symptoms. More generally, it can be defined as a judgment made on a situation, on a state. But the interpretation of the word diagnosis has many meanings depending on the interlocutors to whom it is addressed: the financial diagnosis of a company concerns the verification of its financial state, the medical diagnosis is interested in determining a disease to identify the causes, and the industrial diagnosis, for its part, aims to find the cause of a failure. The medical field quickly adopted diagnostic aid tools.

The implementation of a diagnostic aid system using the medical image goes through several stages: a pre-processing stage, a classification/identification stage, and a final stage for the final decision-making by the medical staff. A radiologist's categorization of breast lesions is a subjective human assessment that can categorize the same lesion in two ways. An automated CAD method, on the other hand, based on the descriptors (characteristics) of the lesion, consistently produces the same results for the same X-ray and so may be used as a reference. To provide a second opinion to the radiologist, an automated Computer Aided Diagnosis system is deployed. Such a system begins with a preprocessing in order to obtain a more readable and less noisy image. This pre-treatment facilitates the task of the following steps. A step of extracting mathematical descriptors allows the classification of tissue type and the detection of the presence of anomaly. Then the final step is to make a decision.

Classification of breast tissue density is an important step. This information will be used for the diagnosis of breast tissue. The concept of systems dedicated to diagnostic assistance CAD has been emerging for about fifteen years. Several teams have taken an interest in automated computer systems to help detect and diagnose radiological lesions in mammography. They are intended for computer reading which is intended to assist but not to substitute for the radiologist. The digital analysis of the mammography images can then serve as a second computer readout for the radiologist. Several recent studies have shown that these CAD systems can increase the rate of cancers detected by 15 to 20% [10].

2.4 Diagnosis/detection support system for mammography

The proposed diagnostic/detection support system for mammography consists of several steps described in the following figure 2.1:

The stages depicted in figure form a diagnostic assistance system for mammography, with the ultimate step allowing for the diagnosis of breast abnormalities [10].

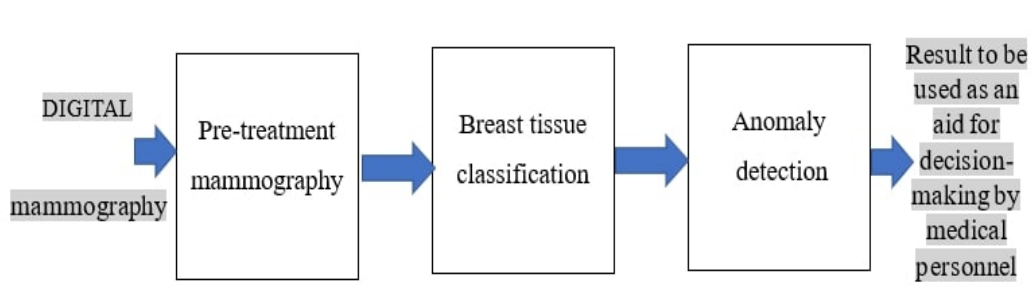


Figure 2.1: The stages of the diagnostic/detection support system for mammography

2.4.1 Mammography Preprocessing

The majority of pixels in an image are redundant and do not add much to the image's inherent information. To prevent extra processing overhead while working with Artificial Intelligence (AI) networks, it is vital to remove them. Compression methods can help with this. We'll start by putting our deep net into action. The photos in the dataset are being processed. This is accomplished with the assistance of Python's implementation of the OpenCV library. There are other different modules that may be utilized. MATLAB or other image processing libraries, for example, were utilized in this stage software this is required to eliminate redundancy in the input data. It only adds to the network's computational complexity without bringing about any meaningful improvements in the outcome.

2.4.2 Classification of breast tissue

The density of breast tissue is an essential characteristic of breast anatomy and physiology. Density is significant for two reasons in particular: To begin with, increasing mammography density is linked to a decrease in mammography sensitivity for detecting breast cancer. Second, breast density is one of the most powerful recognized risk factors for breast cancer in women under the age of 70. For all of these reasons, automated tissue density categorization is an essential diagnostic method. To categorize breast tissue, many classification approaches have been used; the following table 2.1 is a non-exhaustive depiction of this work [10].

Description of the method	Database Used
<p style="text-align: center;">in 2005</p> <p style="text-align: center;">This study presents two methods: the k nearest neighbors algorithm and the decision tree [11].</p>	MIAS
<p style="text-align: center;">in 2006</p> <p style="text-align: center;">a breast density classification technique using a multi-resolution histogram has been proposed [12].</p>	MIAS
<p style="text-align: center;">in 2011</p> <p style="text-align: center;">Several methods have been used for the classification of breast density: - Classification and regression trees - The k nearest neighbors algorithm -Support Vector Machine (SVM) [13].</p>	Mini-MIAS
<p style="text-align: center;">in 2012</p> <p style="text-align: center;">In this article, they propose the use of the naive bayesian classifier and the k nearest neighbors algorithm [14] .</p>	Mini MIAS and KBD-ER digital mammography
<p style="text-align: center;">in 2013</p> <p style="text-align: center;">This article presents a method based on estimating breast density. The overall profile of breast tissue density is represented using a topographic map [15] .</p>	MIAS and DDSM
<p style="text-align: center;">in 2018 has been proposed :</p> <p style="text-align: center;">In the proposed approach, the values deduced from the histogram will be processed by Artificial Neural Networks (ANN) for the breast tissue classification [10].</p>	Mini-MIAS

Table 2.1: Breast tissue density classification methods.

Description of the method	Database Used
<p style="text-align: center;">in 2010 ,</p> <p>An automatic diagnostic aid system is applied to the detection and localization of suspicious areas in mammograms. The proposed algorithm contains three essential steps; in the first step a method based on active contours and the chamfer map is used for the detection of contours of the mammary gland. In the second step a segmentation method is used to segment the pectoral muscle, the aim of the two previous steps is to limit the region of interest, in the third step a genetic active contour is used to locate the regions of suspicious masses [10] .</p>	MIAS
<p style="text-align: center;">in 2012</p> <p>This article presents an approach based on a hybridization of the K-means method and the harmonic search method Harmony Search (HS) in order to detect tumors [16].</p>	Mammographic images of size 256*256
<p style="text-align: center;">in 2015</p> <p>The study proposes a computer-aided diagnostic technique using the hybridization of the genetic algorithm by the GA-PSO particle swarm optimization algorithm, for the selection of texture features. The KNN classifier is used to classify normal and abnormal breast tissue [17].</p>	Mini-MIAS
<p style="text-align: center;">in 2016</p> <p>In this article a Gabor filter is used to calculate characteristics that will be used to select the most relevant pixels. Finally, a classification of breast tissue into two abnormal/normal classes is performed using a SVM [18] .</p>	Mini-MIAS
<p style="text-align: center;">in 2018 has been proposed:</p> <p>The present study proposes an interpretation of mammograms by a system based on an artificial neural network capable of detecting the presence or absence of breast abnormality [10].</p>	Mini-MIAS

Table 2.2: Breast tissue abnormality detection methods.

2.4.3 Detection of an anomaly in Breast tissue

We are going to study the problem of detecting the presence or not of an anomaly in a mammogram, several studies have been carried out for the detection of anomalies table 2.2 [10].

2.5 Convolution neural network

Convolutional Neural Network (CNN)s are a sort of neural network that processes input using a preset grid-like topology. In practical applications, convolutional networks have had a lot of success. The usage of a mathematical procedure known as convolution is referred to as a "convolutional neural network". Convolutional networks, in other words, are neural networks having at least one layer that use convolution rather than traditional matrix multiplication. The biological inspiration for CNNs is the visual cortex in animals. Small sub-regions of the input are sensitive to the visual cortex cells, which is referred to as the visual field (or receptive field). These smaller sub-regions are tiled together to capture the whole visual field. The cells are well-suited to take advantage of the high spatially local correlation evident in the types of images our brains comprehend, acting as local filters across the input space. In this part of the brain, there are two types of cells. Simple cells fire when they detect edge-like patterns, whereas more complex cells fire when they have a bigger receptive field and are unaffected by the pattern's location. CNNs are responsible for major medical imaging discoveries as a consequence of having the upper hand when it comes to dealing with images. Following that, we'll go through the fundamental components of these networks [19].

2.5.1 Input Layers

Input layers are placeholders for picture raw data. The input data is usually three-dimensional, with the width, height, and number of channels specified. The depth or color channels are represented by the latter (three for Red Green Blue (RGB) or just one in the case of greyscale images) [19].

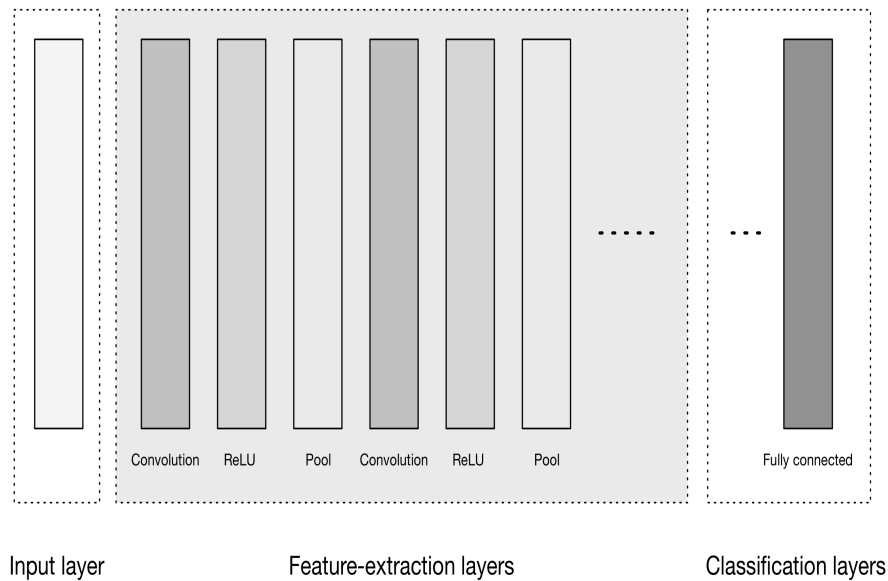


Figure 2.2: A high-level overview of CNN Architecture

2.5.2 Convolutional Layers

Convolutional layers execute a convolution on the input before passing the output to the next layer. A convolution is a technique for converting all of the pixels in a receptive region into a single value. When you apply convolution to a picture, for example, the size of the image is decreased as all of the information in the field is combined into a single pixel. This function is followed by an element-wise non-linear activation function (typically ReLU), which modifies the pixel values while maintaining the input data's spatial dimension [19].

Fourier transformers are a mathematical procedure that allows two sets of data to be combined. The input to a convolution operation is a matrix representing raw data or a feature map from a previous convolution, as shown in the diagram. To create entries in the output feature map, a kernel (also known as a filter) is slid over the input matrix [19].

To create the 3D output volume, the activation maps for each filter are layered along the depth axis.

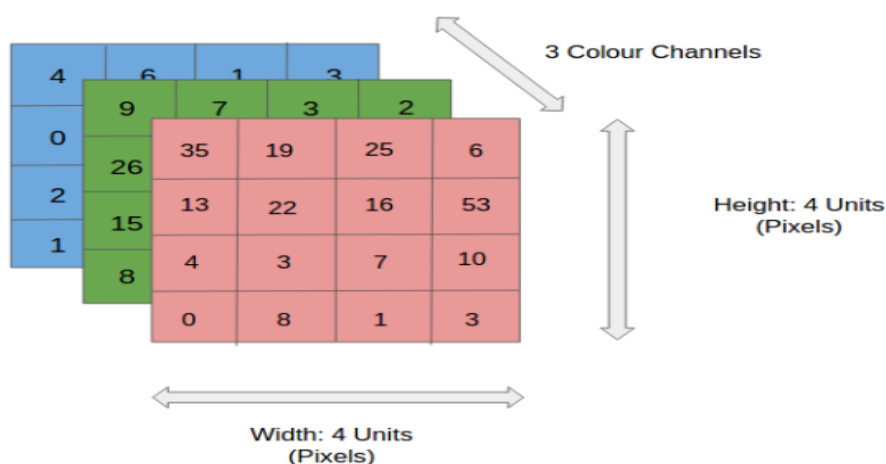


Figure 2.3: Input layer 3D volume

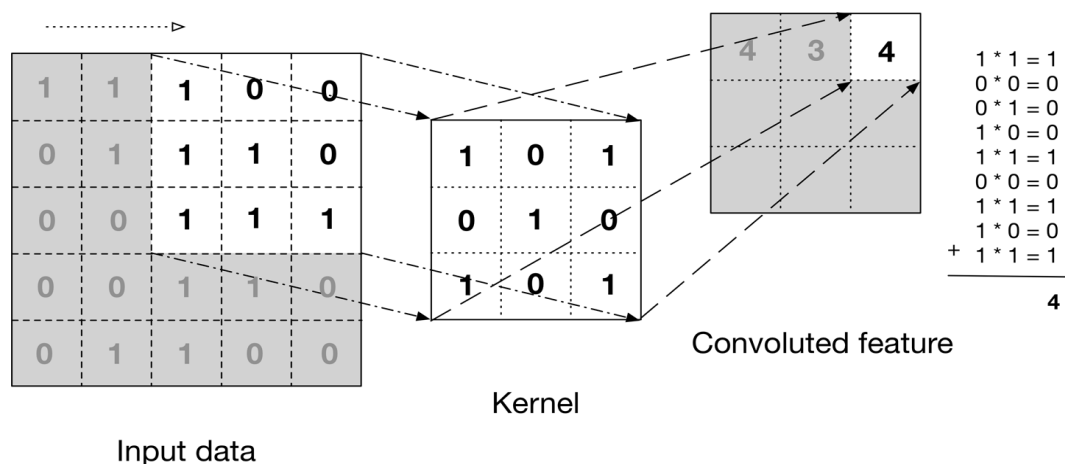


Figure 2.4: The convolution operation.

2.5.3 Pooling Layers

Pooling layers, which are often added between consecutive convolutional layers, are another important basic component in ConvNets. They apply downsampling to the input, gradually reducing the data representation across the network. By summarizing subregions using some statistical function, such as taking the average or maximum value, pooling processes reduce the size of feature maps. One of the most popular pooling filters used in CNN is a 2×2 filter with a stride of 2. This filter down-scales each input depth slice by a factor of two while maintaining spatial correlation [19].

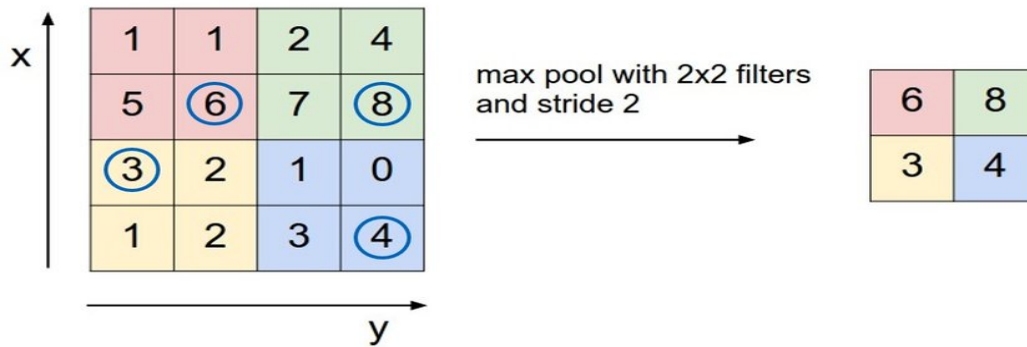


Figure 2.5: Max pooling on a single depth slice using a 2×2 filter with a stride of 2.

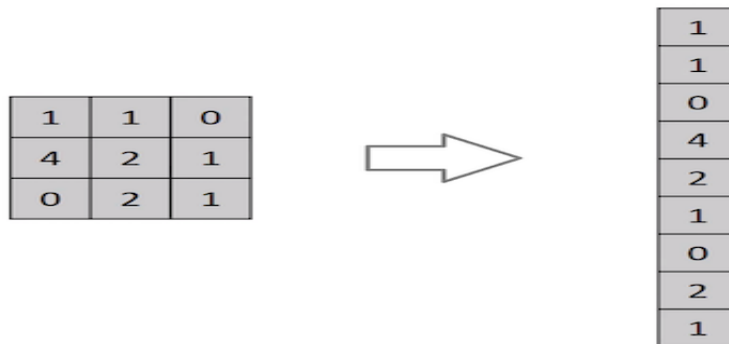


Figure 2.6: The output of the flattening operation is a vector.

2.5.4 Fully Connected Layers

Fully connected layers, also known as feed forward neural networks, are utilized in the last phase of CNN. The final Pooling or Convolutional Layer output is flattened and then provided as input to the fully linked layer. The process of unrolling the values of a three-dimensional matrix into a vector is known as flattening. It's worth noting that the final layer makes use of the Softmax algorithm (instead of Rectified Linear Unit (ReLU)). In the case of a classification task, the last fully connected layer is used to compute class scores. The dimensions of the output volume of the last layer is $[1 \times 1 \times N]$ where N is the number of target classes [19].

2.6 Conclusion

Although breast cancer is the most common disease among women worldwide, and despite its high risk, it can all be avoided by early detection to avoid advanced stages that are difficult for doctors to deal with (treatment). Unlike the detection and diagnosis manual, the often mechanisms of deep learning have given a major impetus to the rapid detection and diagnosis of these tumors.

With human progress, scientists and experts are trying to introduce artificial intelligence in all fields in order to facilitate life and find the best results in the shortest period of time. This could save thousands of lives around the world, The earlier the detection accurately, the more women can avoid breast cancer. With the advancement of science, there are now different types of neural networks such as Recurrent Neural Networks Recurrent Neural Networks (RNN), ANN, and CNN. In our experience, we found that CNN provides the greatest results for early diagnosis of cancer because, despite the anatomical complexities of the breast, it can detect the disease

3

Results and Discussion

3.1 Introduction

Deep learning algorithms, particularly convolution neural networks (CNN's), are particularly well adapted to detecting patterns in pictures and exploiting those patterns to classify them. We will work on four parameters to get the maximum accuracy (number of epochs, patch size, learning rate, and optimizers), and we will adjust these parameters in this chapter until we discover the optimum value of accuracy from the results we found.

3.2 Proposed approach

This research presents and evaluates a deep learning architecture for automated breast cancer diagnosis that combines machine learning and image categorization ideas. Different Deep Neural Network topologies, particularly those tailored to picture data, such as Convolutional Neural Networks, have been described. This took the labeled (benign/malignant) input image and highlighted the visual patterns, then used those patterns to distinguish between non-cancerous and cancer-containing tissue, similar to how digital staining uses a classifier network to highlight image segments important for diagnostic decisions. The RGB color model, which had 2480 healthy samples and 5429 unhealthy ones, was used to teach the CNN (See Fig. 3.1) in below we describe in detail.

3.2.1 Feature extraction

For both human and machine systems, feature learning is a critical phase in the categorization process. According to research, the human brain is more sensitive to forms than computers are to patterns and texture. As a result, feature learning differs greatly between manual and machine learning. Malignant tumors feature big, irregular nuclei or numerous nuclear structures in the visual environment. The cytoplasm undergoes changes as well, with new structures forming or existing ones disappearing. Malignant cells contain a small quantity of cytoplasm and often have vacuoles. The ratio of cytoplasm to nucleus falls in this circumstance. Experts assess all of these traits or algorithms are built to quantify these features in order to automate detection.

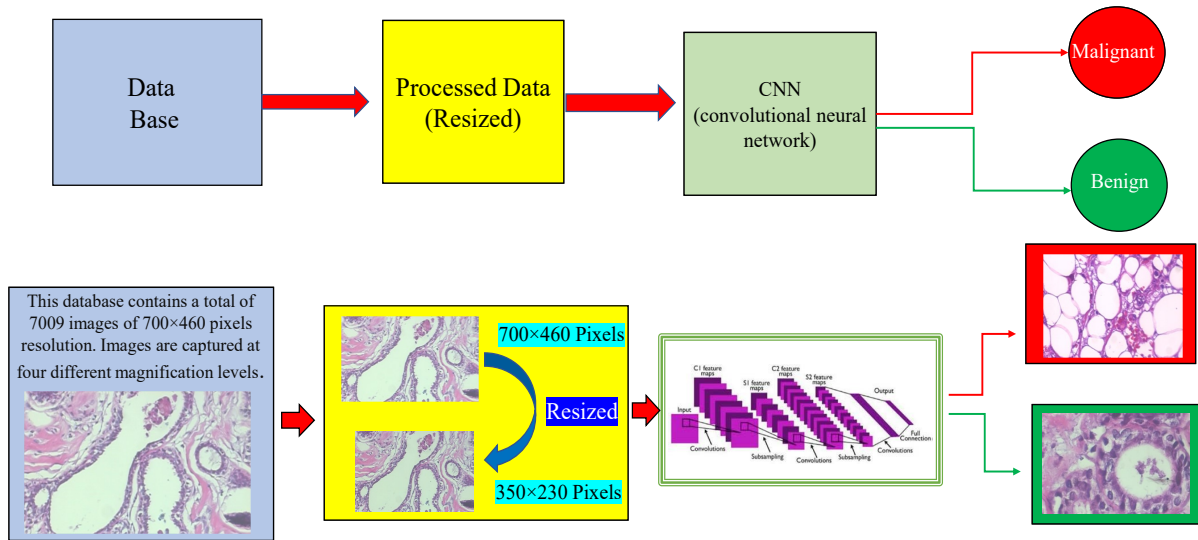


Figure 3.1: The output of the flattening operation is a vector.

Because selection and quantification include a variety of unknown mistakes that are difficult to resolve, this technique is complex and inaccurate. We do not need to give these elements directly in order to oversee learning. In this scenario, photos are given to a CNN-like architecture and their class as a label (Benign or Malignant). From this, CNN can derive computational characteristics from the automated updating of filter values throughout the training phase. In other words, for a particular architecture of CNN filters and their weights, these are attributes that are employed for model assessment during testing. In this method, CNN takes an image’s raw pixels and outputs learning filter weights as shown in figure 3.2 (features learning part).

The details of the network are illustrated in Table 3.1, followed by its visual representation in Fig. 3.2 the number of filters employed in the convolution process increases the depth of the input however, when the pooling layer is applied, the depth remains the same, while the size is reduced. Visual representation of Table 3.1 is shown in Fig. 3.2 ($convX@Y \times Y$) represents convolution with X number of filters of size $(Y \times Y)$, and ($pool@Z \times Z$) represents max pooling with a kernel size of $(Z \times Z)$.

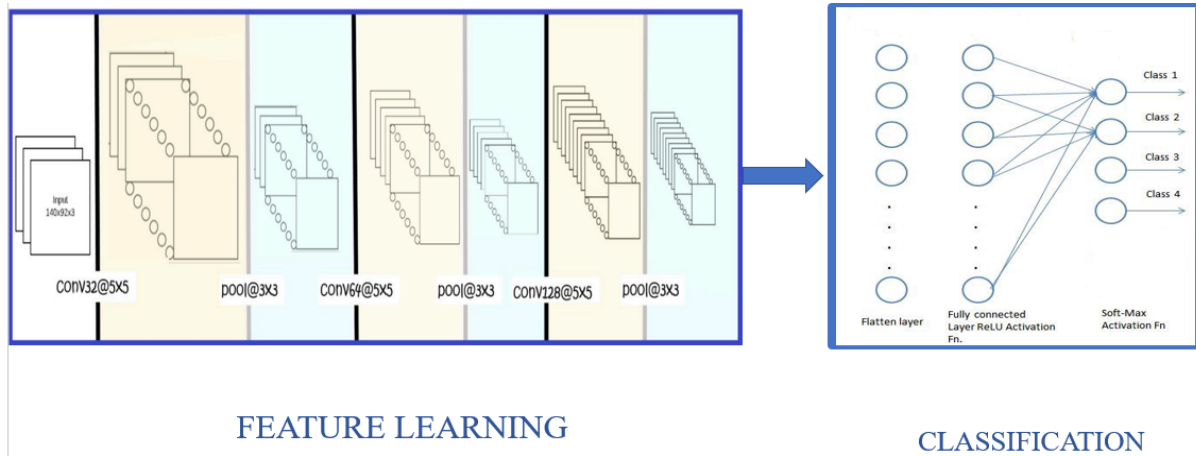


Figure 3.2: CNN Architecture.

Layer attribute	L1	L2	L3	L4	L5	L6
Type	Conv	Pool	Conv	Pool	Conv	Pool
Channel	32	-	64	-	128	-
Filter Size	5x5	-	5x5	-	5x5	-
Conv stride	1x1	-	1x1	-	1x1	-
Pooling size	-	3x3	-	3x3	-	3x3
Pooling stride	-	1x1	-	1x1	-	1x1
Padding size	same	none	-	none	-	none
Activation	ReLu	-	ReLu	-	ReLu	-

Table 3.1: Parameters of the CNN architecture.

3.2.2 Classification

The flattened weighted feature map created from the final pooling layer is utilized as input to the fully connected network, which calculates the loss and updates the weights of the internal hidden nodes accordingly during the classification process. Table 3.2 contains the parameters of these layers. These layers are stacked after preprocessing is done. The output of the last layer is taken as the final output as usual.

Layer Attribute	FC-1	FC-2	FC-3
No of nodes	64	64	2
Activation used	ReLu	ReLu	Softmax

Table 3.2: Details of fully connected network.

3.3 Database and protocol

BreakHis [20] is a library of microscopic biopsy images of aggressive and benign breast cancers. From January to December 2014, photographs were taken using a clinical report¹. The P&D lab is referred to patients who have a clinical sign of breast cancer. Patients suffering from breast tumors at P&D Lab Brazil were invited to participate in the study of breast tumors from January to December 2014. The investigation was approved by a member of the establishment, and all of the patients signed a written consent form.

BreakHis breast tumor tissue collection contains 9,109 images. It was acquired from 82 patients with various magnification factors on the site² (40×, 100×, 200×, and 400×) as shown in figure 3.3. There are 5,429 cancerous and 2,480 benign instances (700 × 460 pixels). This data-set was created at Parana, Brazil, with the help of the P& D lab-Pathological Anatomy and Cytopathology. The breast tumor tissue is freely available for researchers to examine.

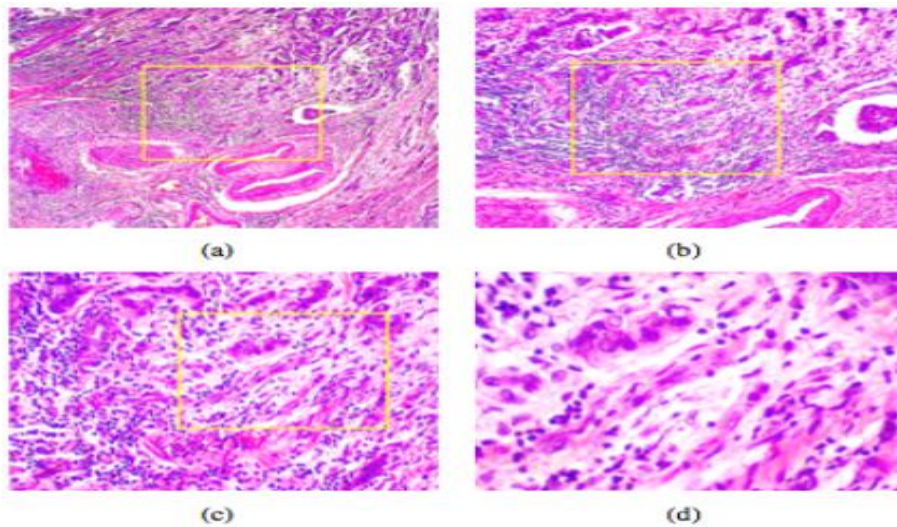


Figure 3.3: Breast malignant tumor slides observed with different magnification ratio 40 X , 100 X , 200 X and 400 X.

The cancers in BreakHis dataset are divided into two categories: benign and malignant tumors. The cause of benign tumors is unknown in general. It grows and divides as the body's cells expand and divide. A benign tumor is a noncancerous tumor that is found in the majority

¹<https://www.wcrf.org/int/cancer-facts-figures/data-specificcancers/breast-cancer-statistics>

²<http://web.inf.ufpr.br/vri/breast-cancer-database>

of women. It does not spread to other organs or areas of the body. Malignant tumor is a term that refers to cancer in general. It spreads to other sections of the body and may result in the person's death. Different biopsy procedures were used to gather samples.

A dataset is a labeled data image that contains all of the details about a patient and the biopsy procedure. Every single image is labeled. The method of biopsy, type of tumor, tumor class, patient identity number, and picture magnification factor are all included in the image. For example, in SOB B TA15-5865-100 001.png, SOB stands for biopsy process, B for benign tumor, and TA for benign tumor of type tubular adenoma, all of which are acquired from slide 15-5865.

Phyllodes tumor (PT), adenosis (A), tubular adenoma (TA), and fibroadenoma (FA) are the four types of benign breast tumor tissue in the database (F). Mucinous carcinoma (MC), lobular carcinoma (LC), papillary carcinoma (PC), and carcinoma are four different types of malignant breast tumors (DC). The distribution of images is detailed in Table 3.3. We used 80% of the data for training and 20% for tests (6,327 images for training and 1582 images for testing).

Magnification	Benign	Malignant	Total
40x	652	1370	1995
100x	644	1437	2081
200x	623	1390	2013
400x	588	1232	1820
Total	2480	5429	7909

Table 3.3: Distribution of images in dataset

3.4 Evaluation metrics

Along with the descriptions of Accuracy (Eq. 3.1), Precision (Eq. 3.2), Recall (Eq. 3.3), and F1-score (Eq. 3.4) numerous terms are widely employed. True positive (TP), True Negative (TN), False Negative (FN), and False Positive (FP) are the four types. The result of a diagnostic test is deemed true positive if a disease is proved to be present in a patient and the offered diagnostic test also reveals the presence of disease. Similarly, if a disease is confirmed to be absent in a patient and the diagnostic test confirms this, the test result is TN. Both true positive

and true negative results indicate that the diagnostic test and the confirmed condition are in agreement (also called the standard of truth). No medical test, however, is without flaws. The diagnostic test result is false positive if it suggests the presence of disease in a patient who does not have it FP. Similarly, if the diagnosis test result indicates that the disease is missing in a patient who has a known ailment, the test result is FN. The terms "false positive" and "false negative" refer to the test findings being the polar opposite of the actual condition.

$$Acc = \frac{TP + TN}{TP + TN + FP + FN} \quad (3.1)$$

$$Precision = \frac{TP}{TP + FP} \quad (3.2)$$

$$Recall = \frac{TP}{TP + FN} \quad (3.3)$$

$$F1 - score = 2 \times \frac{Precision \times Recall}{Precision + Recall} \quad (3.4)$$

Accuracy is the base metric used for model evaluation describing the number of correct predictions over all predictions (See Eq. 3.1). Precision is a measure of how many of the positive predictions made are correct (true positives) (See Eq. 3.2). Recall is a measure of how many of the positive cases the classifier correctly predicted, over all the positive cases in the data (See Eq. 3.3). F1-Score is a metric that combines accuracy and recall. It's often referred to as the harmonic mean of the two. The harmonic mean is a method of calculating a "average" of numbers that is said to be better for ratios (such as accuracy and recall) than the usual arithmetic mean. In this situation (See Eq. 3.4).

3.5 Results and Discussion

In this section, by considering the previously described setup we use some different parameters in CNN architectures to improve the result by focusing on a number of epochs, batch size, learn rate and finally which one is the best optimizer. All these experiments we describe below

in details.

3.5.1 Effectiveness of number epochs

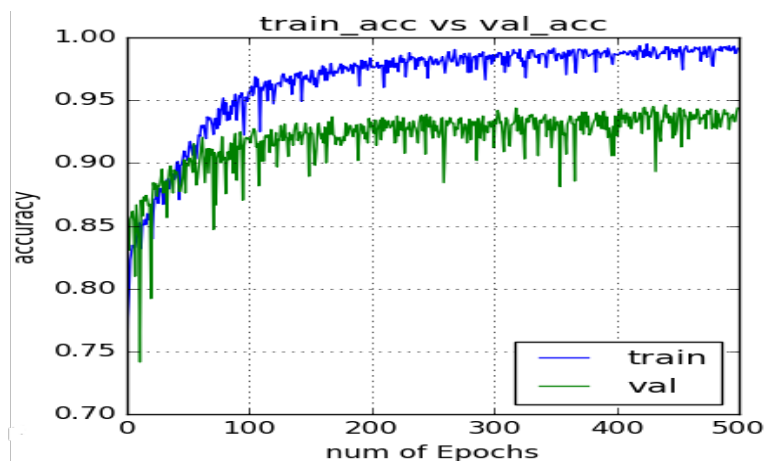


Figure 3.4: Training accuracy and validation accuracy

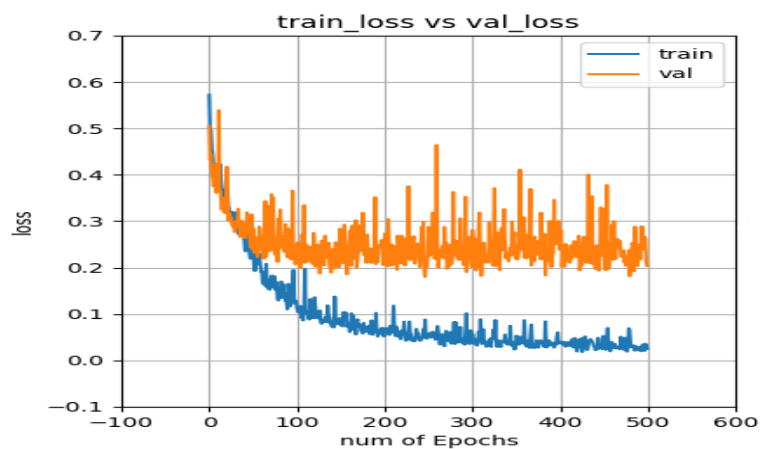


Figure 3.5: Training loss and validation loss

As shown in figure 3.4, the results for accuracy in terms of the number of epochs (in our experiment, 500 epochs) are as follows: we see an increase in accuracy in the range from 1 to 300 epochs, then the accuracy is stable (the highest value possible, 94.37%) in the range from 300 to 500 epochs, and the error rate of validation is the smallest possible value, as shown in figure 3.5, we should stop when the error rate of validation data is the minimum. Consequently, if we

increase the number of epochs, we will have an over-fitted model. In general, too many epochs may cause our model to over-fit the training data. It means that our model does not learn the data, it memorizes the data. So we have to find the accuracy of validation data for each epoch or maybe iteration to investigate whether it over-fits or not, so in our case, we obtained the best accuracy possible of 94.37%.

3.5.2 Effectiveness of Batch size and Learning rate

Batch size is the number of samples processed before the model is updated, and this can help to not wait until the whole data is processed, which may take a long time or even cause further problems. However, dividing your data into mini-batches has proven its efficiency in terms of better accuracy and training speed.

In general, smaller or larger batch size doesn't guarantee better convergence. Batch size is more or less treated as a hyperparameter to tune, keeping in mind the memory constraints you have. There is a tradeoff between bigger and smaller batch sizes, which each have their own disadvantages, making it a hyperparameter to tune in some sense. The theory says that the bigger the batch size, the less the noise in the gradients and the better the gradient estimate. This allows the model to take a better step towards a minimum. And that's what we can notice by setting the batch size bigger than 128 to lose in terms of accuracy. However, the challenge is that a bigger batch size needs more memory, and each step is time-consuming. Even if somehow we could avoid the time and space constraints, a bigger batch size still wouldn't give a better solution in practice compared to a smaller batch size. This is because the surface of the objective of the neural network is generally non-convex, which means that there might be local optimums. Just having an accurate gradient estimate doesn't guarantee us reaching the global optimum (which we seek). It could lead us to a local optimum very accurately! Keeping the batch size small makes the gradient estimate noisy, which might allow us to bypass a local optimum during convergence. This is what happens by increasing our batch size to 256. But having a very small batch size would be too noisy for the model to converge anywhere. That's what we see for batch sizes less than 128. So, the best batch size depends on the network you are training, and the data you are training with, and the objective function you are trying to

Batch size	32		64		128		256	
Accuracy	89.51%		93.92%		94.37%		94.05%	
Precision	Benign	0.94	Benign	0.93	Benign	0.93	Benign	0.93
	Malignant	0.88	Malignant	0.93	Malignant	0.95	Malignant	0.94
	AVG	0.91	AVG	0.925	AVG	0.94	AVG	0.935
recall	Benign	0.71	Benign	0.85	Benign	0.89	Benign	0.88
	Malignant	0.98	Malignant	0.98	Malignant	0.97	Malignant	0.97
	AVG	0.845	AVG	0.915	AVG	0.93	AVG	0.925
F1 score	Benign	0.81	Benign	0.9	Benign	0.91	Benign	0.9
	Malignant	0.93	Malignant	0.96	Malignant	0.96	Malignant	0.96
	AVG	0.87	AVG	0.93	AVG	0.935	AVG	0.93

Table 3.4: Batch size

Learning rate	0.1	0.01	0.001	0.0001
Accuracy	68.20%	68.21%	94.37%	92.48%
Training time	201min17sec	146min35sec	268min46sec	269min01sec

Table 3.5: Learning Rate

optimize. Finally, we found that the optimal batch size to use is 128. This is the batch size we will use in the next experiments. as shown in Table 3.4.

Then, we tried to lookahead how can the learning rate affect our training phase. Actually, The learning rate may be the most important hyperparameter when configuring your neural network. Where in fact, the learning rate is a hyperparameter that controls how much to change the model in response to the estimated error each time the model weights are updated. Choosing the learning rate is challenging as a value too small may result in a long training process that could get stuck, whereas a value too large may result in learning a sub-optimal set of weights too fast or an unstable training process. And here in our experiment, it shows that with a learning rate of 0.01 our model has a better execution time as shown in table 3.5. However, the accuracy is very low which is in fact due to a sub-optimal set of weights. Whereas, a smaller learning rate of 0.001 gives better accuracy but with a longer time.

3.5.3 Effectiveness of optimizer

Optimizers are techniques or strategies for minimizing an error function (loss function) or increasing production efficiency. Optimizers are mathematical functions that are based on the

Optimizers	Adam		Adamax		SGD		RMSprop	
Accuracy	94.37%		93.81%		85.52%		88.94%	
Precision	Benign	0.92	Benign	0.89	Benign	0.84	Benign	0.88
	Malignant	0.95	Malignant	0.96	Malignant	0.86	Malignant	0.89
	AVG	0.935	AVG	0.925	AVG	0.85	AVG	0.885
recall	Benign	0.90	Benign	0.92	Benign	0.68	Benign	0.85
	Malignant	0.96	Malignant	0.95	Malignant	0.94	Malignant	0.89
	AVG	0.93	AVG	0.935	AVG	0.81	AVG	0.87
F1 score	Benign	0.91	Benign	0.90	Benign	0.75	Benign	0.81
	Malignant	0.96	Malignant	0.95	Malignant	0.9	Malignant	0.82
	AVG	0.935	AVG	0.925	AVG	0.825	AVG	0.815

Table 3.6: Optimizers

learnable parameters of a model. Biases and weights optimizers assist in determining how to adjust the weights and learning rate of a neural network in order to minimize losses.

There are several types of optimizers, but we only used four for our experiment (Adam, Adamax, SGD, and RMSprop). Based on the results in the table 3.6, we can see that SGD and RMSprop have the lowest accuracy (85.52% and 88.94%, respectively), while the Adam optimizer has the highest (accuracy = 94.37%) with (a precision = 93.5%, recall = 93%, and F1-score = 93.5%), so we used Adam in our experiment.

3.5.4 Compared with state of the art

The confusion matrix obtained is shown in Fig 3.6, which visually depicts the results of Table 3.7. We may deduce from Fig 3.6 that the Malignant class is the actual class in this situation; hence, the TP, TN, FP, and FN values are 64.97%, 29.23%, 3.24%, and 2.53%, respectively.

	Precision	Recall	F1-score
Benign	0.92	0.90	0.91
Malignant	0.95	0.96	0.96
Avg/total	0.935	0.93	0.935

Table 3.7: Summary of result

We acquired a degree of precision with the aforesaid arrangement that was superior to many state-of-the-art experimental setups. We evaluated our findings (94.37% validation accuracy



Figure 3.6: Confusion matrix.

from the test set) with various published research (Table 3.8) for comparison. Along with the increase in accuracy, there has been a considerable increase in precision (93.5% in our instance, and 63.36% [21] and 90.63% [22] and 93% [23] respectively) and recall (as 93% in our case and 76.67% [21] and 86.39% [22] and 93% [23]) This method is particularly advantageous since the system is totally automated and any user may test a new image.

Year	Method Used	Validation
		Accuracy Range (in %)
2017	K-Nearest Neighbor [22]	83 to 86
2017	Pre-Trained Networks [24]	80 to 89
2017	Feature Extracted Using CNN [25]	83 to 90
2018	Deep Convolution Neural Network [21]	91.54
2019	Cancer diagnosis in histopathological image: CNN based approach [23]	93.45
2022	Deep Neural Networks Improve Radiologists' Performance in Breast Cancer Screening	94.37

Table 3.8: Existing methods and respective Accuracy

3.6 Breast Cancer Detection Interface

In this section after we tested all parameters on the CNN architecture are proposed and fixed the best parameters we implemented a GUI interface (See Fig. 3.7).

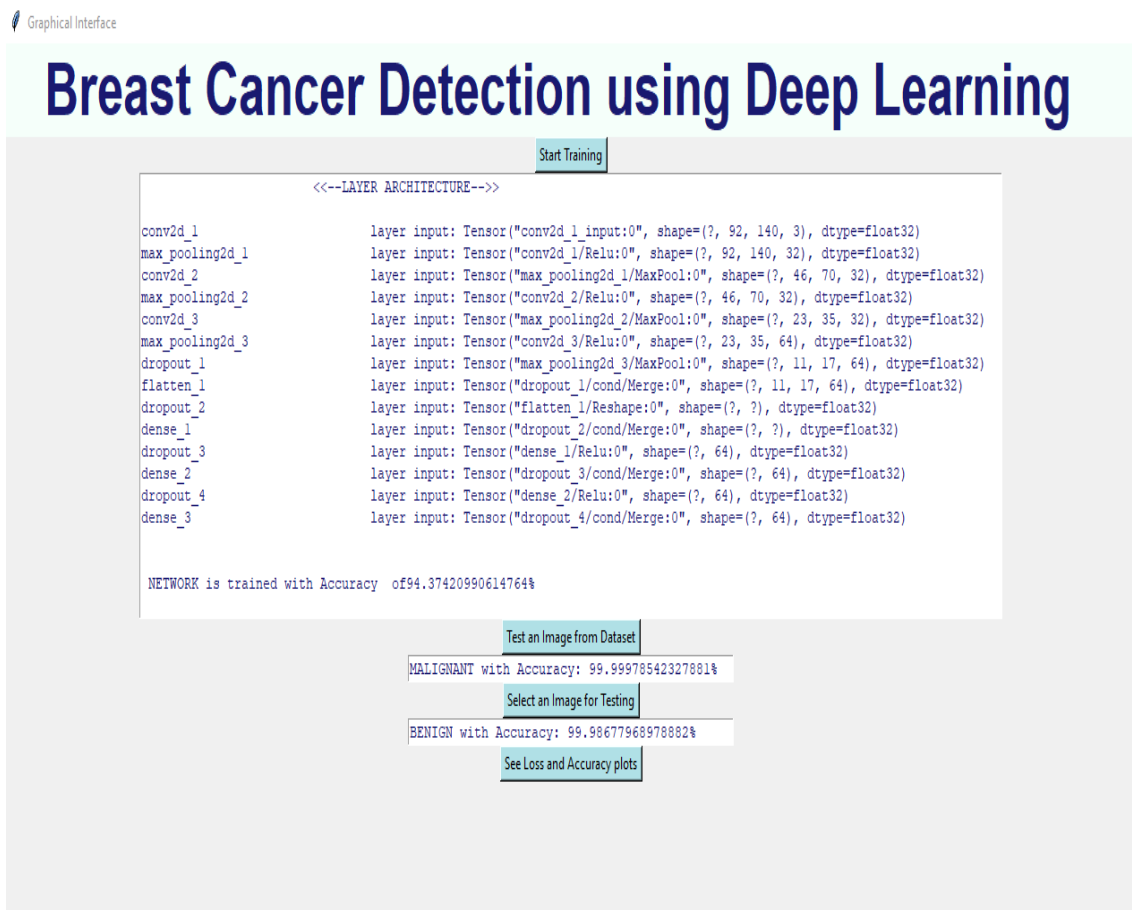


Figure 3.7: Graphical user interface

There is no requirement for domain knowledge even at the design stage because our technique has high prediction accuracy. We evaluated our model with photos of various resolutions of histopathology and found that the findings were mostly unaffected by resolution (refer to Tables 3.9 and 3.10). By using this automated method, it is possible to find cancer early and at a lower cost. This could increase the number of breast cancer patients who survive the disease. We attained the expected result using 7909 biopsy photos of normal and malignant breast tissue in our model with a train-test split of 0.2. Figures 3.8 and 3.9 show the prediction output of four

benign and four malignant photos from the testing set for demonstrative purposes.

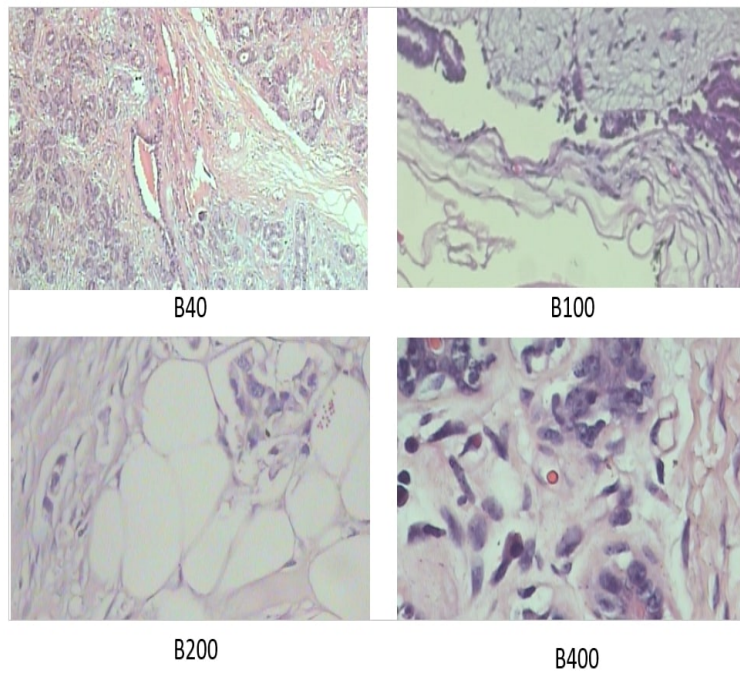


Figure 3.8: Sample Benign image for Testing

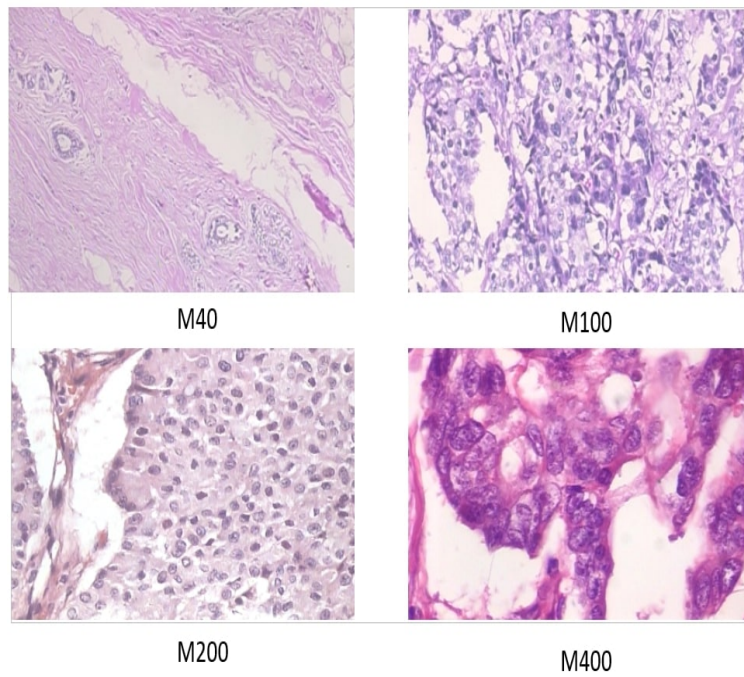


Figure 3.9: Sample Malignant image for Testing

Label	Resolution	Image name in Dataset
B40	40X	SOB_B_A-14-29960CD-40-015.png
B100	100X	SOB_B_PT-14-22704-100-018.png
B200	200X	SOB_B_TA-14-19854C-200-016.png
B400	400X	SOB_B_TA-14-13200-400-008.png
M40	40X	SOB_M_LC-14-12204-40-001.png
M100	100X	SOB_M_LC-14-12204-100-049.png
M200	200X	SOB_M_MC-14-13418DE-200-012.png
M400	400X	SOB_M_PC-14-12465-400-013.png

Table 3.9: Details of sample images from test set.

Label	Actual Class	Predicted Accuracy	Predicted Class
B40	Benign	100%	Benign
B100	Benign	99.99%	Benign
B200	Benign	99.99%	Benign
B400	Benign	99.99%	Benign
M40	Malignant	100%	Malignant
M100	Malignant	99.99%	Malignant
M200	Malignant	99.99%	Malignant
M400	Malignant	99.99%	Malignant

Table 3.10: Prediction result

3.7 Conclusion

In this chapter, we studied and evaluated the latest methods and architectures proposed by recent research on the use of deep learning for the effective diagnosis of breast cancer based on datasets consisting of medical images, especially breast X-ray images, since they were identified as the best imaging modality for this type of detection. Most of the studied architectures could more or less achieve satisfying results with high accuracy. But more research with new and large datasets is always needed to improve the performance of the methods that are already in place and get better results.

General Conclusion

Because breast cancer is one of the most dangerous diseases that affects women around the world, and because it is the leading cause of death in the world due to the slowness with which it is detected or errors in detection, it is necessary to assist specialists doctors by relying on machine learning techniques now more than ever.

Deep learning and specifically convolutional neural networks are considered to be a powerful tool when it comes to image processing because of their ability to recognize spatial information.

ConvNets have demonstrated excellent achievements in both academic and real-world applications, particularly in light of the tremendous increase in computer capacity we've seen in the previous decade. Because x-ray equipment are widely available and even portable nowadays, using X-rays as an imaging modality for detecting cancer may make this technology more accessible in third-world nations. When combined with a rapid, trustworthy, and understandable diagnosis AI helper model, medical teams can save time and money in the fight against this terrible pandemic.

Bibliography

- [1] R. Agarwal *et al.*, “Computer aided detection for breast lesion in ultrasound and mammography,” 2019.
- [2] “Illustration showing the breast anatomy.” [Online]. Available: <https://www.mskcc.org/cancer-care/types/breast/anatomy-breast>
- [3] S. Lei, R. Zheng, S. Zhang, S. Wang, R. Chen, K. Sun, H. Zeng, J. Zhou, and W. Wei, “Global patterns of breast cancer incidence and mortality: A population-based cancer registry data analysis from 2000 to 2020,” *Cancer Communications*, vol. 41, no. 11, pp. 1183–1194, 2021.
- [4] “Mammography system.” [Online]. Available: <https://radiologykey.com/breast-imaging-mammography/>
- [5] “Impacts in mammography.” [Online]. Available: <https://www.mayoclinic.org/tests-procedures/mammogram/about/pac-20384806>
- [6] A. Oliver i Malagelada *et al.*, *Automatic mass segmentation in mammographic images*. Universitat de Girona, 2007.
- [7] E. A. Berns, R. E. Hendrick, M. Solari, L. Barke, D. Reddy, J. Wolfman, L. Segal, P. DeLeon, S. Benjamin, and L. Willis, “Digital and screen-film mammography: comparison of image acquisition and interpretation times,” *American Journal of Roentgenology*, vol. 187, no. 1, pp. 38–41, 2006.
- [8] D. Avrin, R. Morin, D. Piraino, A. Rowberg, N. Detorie, M. Zuley, J. A. Seibert, and E. D. Pisano, “Storage, transmission, and retrieval of digital mammography, including recommendations on image compression,” *Journal of the American College of Radiology*, vol. 3, no. 8, pp. 609–614, 2006.

-
- [9] K. Dingemans, “The effectiveness of breast cancer screening,” Master’s thesis, Sep. 2013. [Online]. Available: <http://hdl.handle.net/2105/14616>
- [10] B. M. EL HABIB, “Application des réseaux de neurones artificiels pour la classification automatique des tissus mammaires,” Ph.D. dissertation, Université de Mostaganem, 2018.
- [11] A. Oliver, J. Freixenet, A. Bosch, D. Raba, and R. Zwigelaar, “Automatic classification of breast tissue,” in *Iberian Conference on Pattern Recognition and Image Analysis*. Springer, 2005, pp. 431–438.
- [12] I. Muhimmah and R. Zwigelaar, “Mammographic density classification using multiresolution histogram information,” in *Proceedings of the International Special Topic Conference on Information Technology in Biomedicine, ITAB*. Citeseer, 2006, pp. 26–28.
- [13] S. D. Tzikopoulos, M. E. Mavroforakis, H. V. Georgiou, N. Dimitropoulos, and S. Theodoridis, “A fully automated scheme for mammographic segmentation and classification based on breast density and asymmetry,” *computer methods and programs in biomedicine*, vol. 102, no. 1, pp. 47–63, 2011.
- [14] M. Muštra, M. Grgić, and K. Delač, “Breast density classification using multiple feature selection,” *automatika*, vol. 53, no. 4, pp. 362–372, 2012.
- [15] Z. Chen, A. Oliver, E. Denton, and R. Zwigelaar, “Automated mammographic risk classification based on breast density estimation,” in *Iberian Conference on Pattern Recognition and Image Analysis*. Springer, 2013, pp. 237–244.
- [16] H. Rahli and N. Benamrane, “Interpretation des images de mammographie par l’algorithme search harmony,” *Annals. Computer Science Series*, vol. 10, no. 2, 2012.
- [17] S. Sundaravinayagam and B. Sankari, “Detection and classification of masses in mammograms using a hybrid ga-pso-knn approach,” *International Journal of Advanced Research Trends in Engineering and Technology*, vol. 2, no. 5, pp. 36–40, 2015.
- [18] J. Torrents-Barrena, D. Puig, J. Melendez, and A. Valls, “Computer-aided diagnosis of breast cancer via gabor wavelet bank and binary-class svm in mammographic images,” *Journal of Experimental & Theoretical Artificial Intelligence*, vol. 28, no. 1-2, pp. 295–311, 2016.
- [19] O. Azzaz Rahmani and M. Taguiouine, “Ai-based decision support system for pulmonary diseases using deep learning techniques for computer vision,” Ph.D. dissertation, 2021.

-
- [20] F. A. Spanhol, L. S. Oliveira, C. Petitjean, and L. Heutte, “A dataset for breast cancer histopathological image classification,” *IEEE Transactions on Biomedical Engineering*, vol. 63, no. 7, pp. 1455–1462, 2016.
- [21] M. Sokolova, N. Japkowicz, and S. Szpakowicz, “Beyond accuracy, f-score and roc: a family of discriminant measures for performance evaluation,” in *Australasian joint conference on artificial intelligence*. Springer, 2006, pp. 1015–1021.
- [22] A. A. Samah, M. F. A. Fauzi, and S. Mansor, “Classification of benign and malignant tumors in histopathology images,” in *2017 IEEE International Conference on Signal and Image Processing Applications (ICSIPA)*. IEEE, 2017, pp. 102–106.
- [23] S. Dabeer, M. M. Khan, and S. Islam, “Cancer diagnosis in histopathological image: Cnn based approach,” *Informatics in Medicine Unlocked*, vol. 16, p. 100231, 2019.
- [24] J. Sun and A. Binder, “Comparison of deep learning architectures for h&e histopathology images,” in *2017 IEEE Conference on Big Data and Analytics (ICBDA)*. IEEE, 2017, pp. 43–48.
- [25] Y. Song, J. J. Zou, H. Chang, and W. Cai, “Adapting fisher vectors for histopathology image classification,” in *2017 IEEE 14th International Symposium on Biomedical Imaging (ISBI 2017)*. IEEE, 2017, pp. 600–603.